MEDICAL PHYSICS International

Proceedings

Books of Abstracts:

- 1. Middle East Medical Physics Conference 08 10 February 2025; Kuwait.
- 2. ICTP Master of Medical Physics Programme 10th Cycle (2022 2024); Trieste, Italy.





The Journal of the International Organization for Medical Physics (IOMP)

MPI Proceedings - Volume 1, Number 1; October 2025



MEDICAL PHYSICS INTERNATIONAL PROCEEDINGS

THE JOURNAL OF

THE INTERNATIONAL ORGANIZATION FOR MEDICAL PHYSICS



MEDICAL PHYSICS INTERNATIONAL Proceedings, Vol. 1, No. 1; 2025

MEDICAL PHYSICS INTERNATIONAL

The Journal of the International Organization for Medical Physics

Aims and Coverage:

Medical Physics International (MPI) is the official IOMP journal. The MPI Proceedings provides a platform for medical physicists to share their experience, ideas and new information generated from conference abstracts/proceedings, and dissertation abstracts for recent graduates in medical physics or closely related fields. The e-journal is available free of charge to IOMP members.

MPI Co-Editors in Chief

Francis Hasford (Ghana) and Sameer Tipnis (USA)

MPI Editorial Board

John Damilakis, IOMP President (2022-2025), EFOMP Past-President, Greece

Eva Bezak, IOMP Vice-President (2022-2025), AFOMP President, Australia

Magdalena Stoeva, IOMP Secretary General (2022-2025)

Ibrahim Duhaini, IOMP Treasurer (2022-2025), MEFOMP Past-President, Lebanon

Mahadevappa Mahesh, IOMP Scientific Comm. Chair (2022-2025); AAPM President-Elect, USA

Simone Kodlulovich Renha, IOMP Professional Relations Comm Chair (2022-2025), ALFIM Past-President, Brazil

Arun Chougule, IOMP Education & Training Comm Chair (2022-2025), AFOMP Past-President, India

Kwan Ng, IOMP Awards and Honours Committee Chair (2022-2025), SEAFOMP Past President, Malaisia

Chai Hong Yeong, IOMP Medical Physics World Board Chair (2022-2025), Malaysia

Hassan Kharita, IOMP Publications Committee Vice Chair (2022-2025), MEFOMP Vice-President, Syria

KY Cheung, IOMP Past-President, Hong Kong, China

Chris Trauernicht, FAMPO Past-President, South Africa

Taofeeq Ige, FAMPO Past-President, Nigeria

Marco Brambilla, EFOMP Past-President, Italy

Anchali Krisanachinda, SEAFOMP Past-President, Thailand

Renato Padovani, EFOMP Past Secretary General, ICTP, Italy

Colin Orton, IOMP Past-President; AAPM Past-President, USA

MPI Founding Editors in Chief: Slavik Tabakov (IOMP Past-President) and Perry Sprawls

MPI History Edition Editors: Slavik Tabakov, Perry Sprawls, Geoffrey Ibbott

MPI web address: www.mpijournal.org

Published by: The International Organization for Medical Physics (IOMP); Web address: www.iomp.org ; Post address: IOMP c/o IPEM, 230 Tadcaster Road, York YO24 1ES, UK.

Copyright ©2013 International Organisation Medical Physics. All rights reserved. No part of this publication may be reproduced, stored, transmitted or disseminated in any form, or by any means, without prior permission from the Editors-in-Chief of the Journal, to whom all request to reproduce copyright material should be directed in writing. All opinions expressed in the Medical Physics International Journal are those of the respective authors and not the Publisher. The Editorial Board makes every effort to ensure the information and data contained in this Journal are as accurate as possible at the time of going to press. However, IOMP makes no warranties as to the accuracy, completeness or suitability for any purpose of the content and disclaim all such representations and warranties whether expressed or implied.

ISSN 2306 - 4609

CONTENTS

EDIT	ORIA	LS	
	EDI	TORIAL FROM CO-EDITORS-IN-CHIEF	5
	Fra	ncis Hasford & Sameer Tipnis	
воо	K OF	ABSTRACTS	
	MII	DDLE EAST MEDICAL PHYSICS CONFERENCE (MEFOMP 2025); 08 – 10 February 2025; Kuwait.	6
	1.	N. Al Maymani, R. Al Mamari, A. Al Jabri, S. Kheruka, N. Al Makhmari, H. Al Saidi, S. Al Rashdi, A. Al Balushi; Comparative Assessment of Average Glandular Dose in Digital Breast Tomosynthesis and Full-Field Digital Mammography in Oman	8
	2.	N. Hasan, S. Alkhazzam, M. Kharita; Evaluation of Mammography Equipment Performance: A Comparative Study of Three Automatic Protocols	9
	3.	A. Al Attar, S. Al Manea, C.M. De Castro, M.H. Kharita; Radiation Dose Monitoring of Dental Radiology Workers at Hamad Medical Corporation: A Five-Year Analysis (2020–2024)	11
	4.	R. Al Maashani, A. Al Maawali, A. Al Maimani, H. Nadeem, A. Al Jabri, Y. Bouchareb; Extraction, Selection and Comparison of Radiomic Features from Cardiac Rest and Stress SPECT/CT scans	13
	5.	A. Al Rahim Alaa, G. Amer, A. Souha, T. Tarraf, H. Rabih, M.H. Kharita, F. Hadi; CT-less PET Attenuation Correction Using Artificial Intelligence	14
	6.	H.J. Alwadai, L.A. Al Mubarak, M.A. Alqahtani, T.A. Alrebdi; A Retrospective Study of High-Dose-Rate Brachytherapy for Cervical Cancer Treatment Using 3D Printed Applicators: A Comparative Analysis with Conventional Applicators at KFMC In Riyadh	16
	7.	S. Alkhazzam, and M.H. Kharita; Identifying Human Errors in Automated Radiographic Quality Control Systems using Advanced Power Business Intelligence	17
	8.	S. Alkhazzam, and M.H. Kharita; Performance of the Shielding of Radiation Protection Gloves using Hand Anthropomorphic Phantom	19
	9.	M. Alfishawy, N. Babu, I. Al Amri, M. Gurumani, Z. Al Mandhari; The Influence of VMAT and Treatment Site on Radiation Use Factor Determination	20
		M. Yaseen, T. Nishtar, R. Ajaj, A. Ali; Enhancing Patient Safety Through Radiograph Rejection Analysis: Insights from a Diagnostic Imaging Department Audit	21
		A. Ayadi, B.O. Mdimagh, C.I. Hammami; Lung Cancer Segmentation with a U-Net Architecture for Improved Tumor Diagnosis, Treatment Planning, and Radiotherapy	22
		K. Somarathne, G. Muthumali, K. Dhanaraj, S. Welarathna, B. Hewavithana, S. Sarasanandarajah, S. Velautham; Breast Size-Based Typical Values in Mammography: A Case Study in Sri Lanka	23
		A. Ghujeh, H. Fayad, A. Abd Al Rahim, A. AlAttar, M. Kharita; Radiation Dose Monitoring of Nuclear Medicine Department Staff: A Five-Year Analysis (2020-2024)	24
		H.H. Alabedi, M.A. Alrawi, N.M. Ali, M.S. Almusawi, R. Ahmad; The Impact of the Half-Life of Fluorine-18 Depending on the Purity Level of Heavy Water on the Image Quality of PET-Scan Imaging	25
	15.	S. Welarathna, S. Viswakula, V. Sivakumar, S. Sarasanandarajah; Regression-Based Machine Learning for Dose Prediction and Optimization in Chest X-Ray Examinations	27
	16.	S. Al-Rawahi, S. Kheruka, N. Al-Maymani, N. Al-Makhmari, H. Al-Saidi, S. Al-Rashdi, A. Al-Balushi, K. Al-Riyami, R. Al-Sukaiti; Evaluation Of Noise-Equivalent Counts and Signal-to-Noise Ratio in (18)F-FDG PET/CT Reconstruction Methods: A Comparative Study of TOF, TOF+PSF, and PSF-only Techniques	29
	17.	A. Ali, M. Yaseen, R. Ajaj, T. Nishtar, K. Rehman; Assessment of Occupational Doses to Radiation Workers at Lady Reading Hospital, Peshawar, Pakistan (2017-2023)	30
	18.	A. Al-Balushi, N. Al-Maymany, S. Kheruka, H. Al-Saidi, K. Al-Riyami; A Dosimetric Analysis of Organs at Risk for Patients Treated with ¹⁷⁷ LU-PSMA	31
	19.	Y. Lahfi, N. Alkerdi, T. Ayach; Influence of Patient Body Surface Area on the Self-Attenuation Factor of the Patient Body in ¹⁸ F-FDG PET-CT Scans: A Pilot Study	32
	20.	H. Al Saidi, B. Al Abri, A. Al Bulushi, A.Z. Al Kindi, S. Al Rashdi, N. Al Maymani, N. Al Makhmari, S. Kheruka; Optimal Home Isolation Duration for Differentiated Thyroid Carcinoma Patients Treated with High-Dose I-131	33
	21.	M. Al-Abedi, N. Alsaedi, N. Ibrahim, D. Abualsaud, H. Aljamei, A. Alumair, E. Alwuhaib, A. Albuali; Reducing Radiation Dose in PET/CT Imaging without Compromising Quality	34
	22.	A. Aly, A. Barah, I. Tsalafoutas, H. Al Hammar, A. Omar, M. H. Kharita; Investigation of Alert Levels in Interventional Radiology Procedures Performed in Hamad Medical Corporation	35
	23.	A. Aly, R. Shwikani, O. Bobes, M. Al Homaid, C. Mark, A. AlAttar, R. Abdul Rahman, H. Gaili, D. Lemma, N. Sahid, S.M. Al Manea, M.H. Kharita; Indoor Radon Measurement in Some Hamad Medical Corporation Hospitals: Base Line Data	36

	24.	A. Ali, M. Yaseen, S. Burki, R. Ajaj; Establishment of Local Diagnostic Reference Levels (LDRL's) for Fluoro Guided Interventional Radiology Procedures: Single Facility Study at Lady Reading Hospital, Peshawar Pakistan	38
	25.	H. Juma, E. Addison, F. Hasford; Comparative Analysis of 3DCRT and IMRT Treating Plan Techniques in Radiotherapy for Cervical Cancer in Ghana: A Case Study of Komfo Anokye Teaching Hospital (KATH)	40
	26.	M. Najem; Developing an Independent MU Check Script for Cyberknife Plans	41
		M. Najem; Implementation of Open-Source QC Management Web Application "QATRACK+" for Routine QA of	42
		Radiotherapy Equipment	
	28.	M.S. Bagahezel, M.Z. Abdul Aziz, G.K. Appalanaido, S. Mansor; Evaluating the Radiological Characteristics and Tissue Equivalence of Polylactic Acid (PLA)-Based Three-Dimensional Printing Filaments for Radiotherapy	43
	29.	B.S. Sesath, J.H.J.K. De Silva, P. Alahakoon; Dosimetric Feasibility of Fast Forward Breast Radiotherapy using Co-60 for Right-Sided Breast Cancer in a Resource Limited Setting	44
	30.	A. Azalmad, Y. Elmaadaoui, M. Hilal; Enhancing Radiotherapy Precision for Cervical Cancer: Minimizing Setup Errors and Refining PTV Margins	45
	31.	S. Weerathunga, S. Welarathna, B. Perera, P. Malge, T. Bandaranayake, S. Rajamanthri, S. Velautham; Investigation of Dose Variation in Adult Non-Contrast Head CT for Radiation Therapy Planning: A Case Study from Sri Lanka	46
	32.	K.V. Anju, M.S. Sreejesh, K. Chiranjib, N. Vijayaprabhu, H.P. Yadav, D. Sharma, V. Subramani, S. Alobaidli;	47
		Development of a Novel 3D-Printed Heterogeneous Phantom for Liver SBRT Dose Verification in Hepatocellular	
		Carcinoma (HCC) Treatment	
	33.	A. Koozari, M. Elhaie, I. Abedi; YOLOv8s-Based Detection of Prostate Cancer Using Multi-Parametric MRI	48
воо	КОБ	ABSTRACTS	
		P MASTER OF MEDICAL PHYSICS PROGRAMME; 10 th Cycle (2022 – 2024); Trieste, Italy.	49
	1.	Tasnim Al Raii; Red bone marrow dosimetry in Lu-177 Dotatate peptide receptor radionuclide therapy using	54
	_	SPECT-CT imaging	
	2.	Ilmude C.N; Comparison between intensity-modulated radiotherapy and volumetric modulated arc therapy using simultaneously integrated boost in head and neck cancer treatment	55
	3.	Astanakulov Rukhiddin; Commissioning and clinical dosimetry calibration of a SPECT/CT scanner	56
	4.	Mukhriddin Barotov; Evaluation and comparison of performances between mammographic machines installed in three different centres, dedicated to clinic and screening	57
	5.	Marufjon Begijonov; Radiotherapy Treatment Optimization in Patients with Stomach Cancer: A Comparison of Rival Plans	58
	6.	Hanna Brynkevich; Evaluation of the dose rate and field size dependence of a liquid filled ionization chamber matrix for pre-treatment verification of stereotactic radiation therapy plan	59
	7.	Guram Chechelashvili; Establishing reliability in radiotherapy, comprehensive LINAC commissioning and TPS beam model validation	60
	8.	Sharon L. GómezVillegas; Optimization of counting statistics in nuclear cardiology studies with a solid-state	61
	٥	detector gamma camera Kanatbek Karauzokov; Image quality in CT: two different approaches for entry-level and advanced evaluation	62
	9. 10	Jerome Kenfac Makeng; Clinical commissioning of four Varian TrueBeam Linacs: an experience from a single	63
	10.	multi-site institution	03
	11.	Javin H. Luke; Development of an updated quality control protocol (QCP) for fixed-type digital Xray equipment managed by Ospedale di Circolo e Fondazione Macchi, Varese, Italy	64
	12.	Aaron Fulgence Mayima Mboungou; Optimization of a quantitative SPECT/CT reconstruction protocol: phantom measurements and preliminary clinical evaluation	65
	13.	Mohammad Mehrpouyan; Stereotactic Body Radiotherapy Treatment for Bone Metastasis: An End-to-End	66
	14.	Study Linda Mission; In vivo evaluation of noise magnitude in Liver CT imaging and how it is influenced by patient	67
	1 -	diameter across different CT scanners and protocols	40
		Eliza Nurlan kyzy, Calibration of linear accelerator with various ionization chambers Adam Superville; Development and Validation of a Software Comparison Framework: An Empirical Analysis of	68 60
		the Monaco and Raystation TPS	69
	17.	Lesly Tsoptio; Commissioning of a new Linac Versa HD for VMAT Treatments	70
INFO	RMA	TION FOR AUTHORS	72

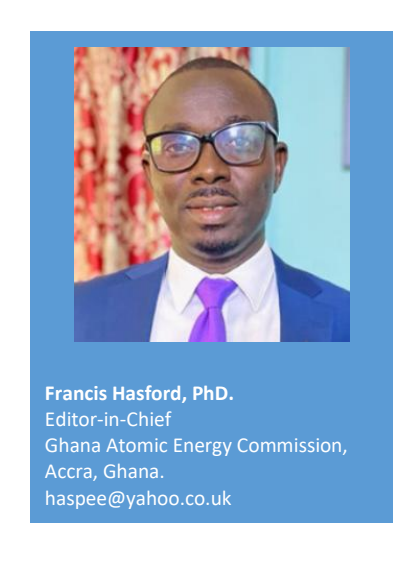
EDITORIAL FROM CO-EDITORS-IN-CHIEF

Francis Hasford & Sameer Tipnis

The IOMP's Medical Physics International (MPI) Journal has remained IOMP's flagship publication since formation in 2013. Since taking over the editorial responsibility from Dr. Slavik Tabakov and Dr. Perry Sprawls, we have produced several issues, keeping the spirit of this publication in mind. The July 2023 issue (Vol. 11, No. 1) compiled over 280 pages including abstracts from the Regional Conference of the Federation of African Medical Physics Organizations (FAMPO) in Morocco in 2022, and the Regional Conference of the Middle East Federation of Medical Physics (MEFOMP) in Oman in 2023. The December 2023 issue (Vol. 11, No. 2) expanded further, featuring abstracts from International Conference on Medical Physics (ICMP) 2023 in Mumbai and theses from the ICTP Master of Medical Physics Programme, reaching a record 618 pages.

By 2024, readership had grown significantly, with the MPI website attracting over 1,000 daily visits at peak. To manage the expanding content, the Publications Committee initiated the establishment of MPI-Proceedings, a special series dedicated to books of abstracts from ICMPs and World Congresses. This innovation is to ensure consistency in archiving, and to build MPI into a family of journals that includes MPI, MPI-History Edition, MPI-Proceedings, etc.

This maiden issue of the MPI-Proceedings publishes abstracts from the Middle East Medical Physics Conference (MEFOMP 2025) held in Kuwait, from 08 – 10 February 2025, and the dissertation abstracts from the 10th Cycle (2022 – 2024 batch) of the ICTP Master of Medical Physics Programme, Trieste, Italy. Enjoy reading MPI-Proceedings and share with us your feedback, if you may.





	MEDICAL PHYSICS INTERNATIONAL Proceedings, Vol 1, No. 1; 2025
	A DOTD A CTC OF THE
	ABSTRACTS OF THE
MIDDLE	E EAST MEDICAL PHYSICS CONFERENC
	(MEEOMD 2025)
	(MEFOMP 2025)
	08 – 10 February 2025, Kuwait









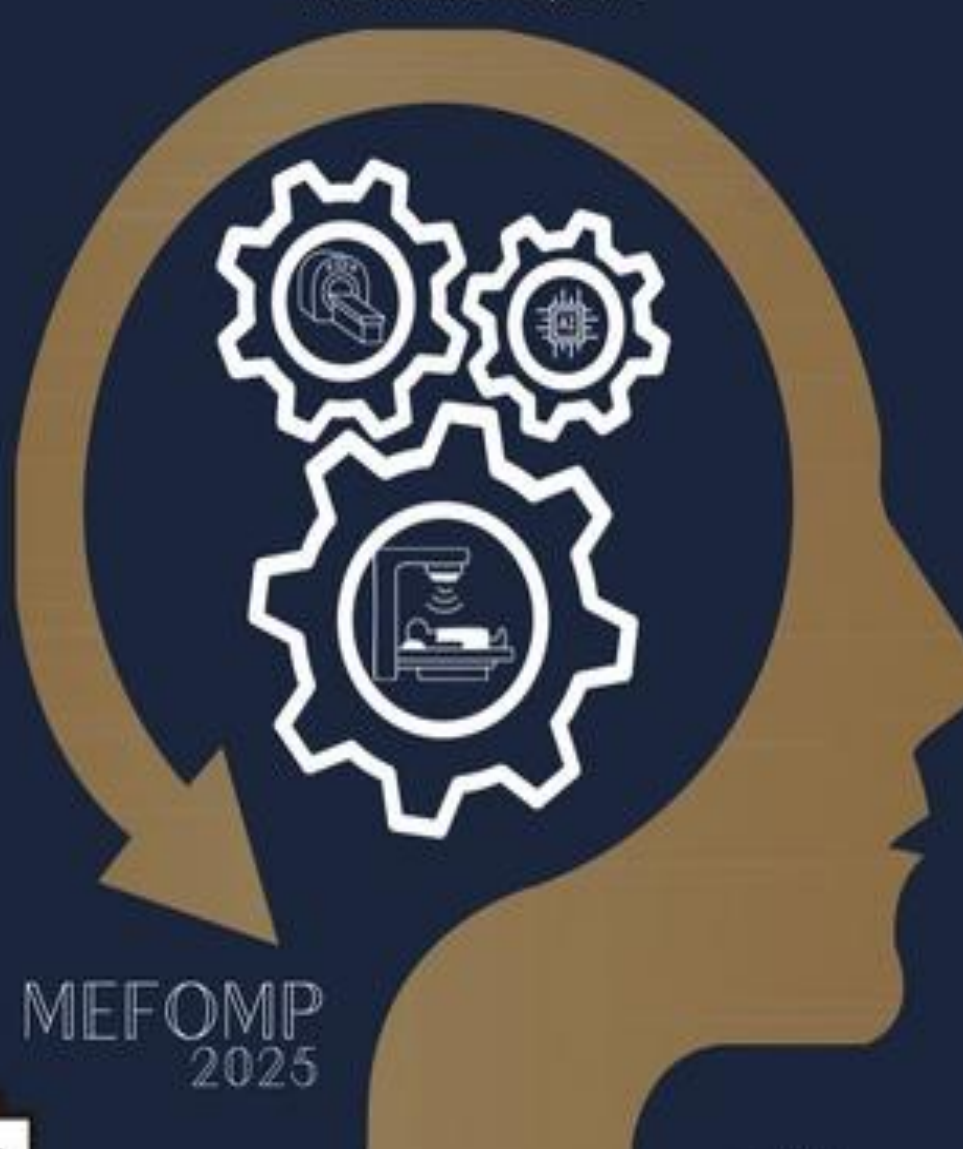




MIDDLE EAST

MEDICAL PHYSICS CONFERENCE

FEBRAUARY 8-10, 2025



SCAN ME



www.mefamp-conference.com

22 CME Category 1

CPD Category 1



COMPARATIVE ASSESSMENT OF AVERAGE GLANDULAR DOSE IN DIGITAL BREAST TOMOSYNTHESIS AND FULL-FIELD DIGITAL MAMMOGRAPHY IN OMAN

N. Al Maymani¹, R. Al Mamari², A. Al Jabri³, S. Kheruka¹, N. Al Makhmari¹, H. Al Saidi¹, S. Al Rashdi¹, A. Al Balushi¹

ABSTRACT

Background: With the integration of Digital Breast Tomosynthesis (DBT) into breast imaging, there has been a significant advancement in the capabilities of Full-Field Digital Mammography (FFDM) for early breast cancer detection. However, the increased use of DBT raises concerns regarding radiation exposure levels.

Objective: This study seeks to determine diagnostic reference levels (DRLs) at the Sultan Qaboos Comprehensive Cancer Care and Research Centre (SQCCCRC) for both FFDM and DBT across different compressed breast thicknesses (CBT), contributing to enhanced understanding of radiation dosimetry in breast cancer diagnosis.

Methodology: Data including average glandular dose (AGD), kVp, mAs, entrance surface dose (ESD) and CBT were retrospectively collected on FFDM and DBT exams. For seven CBT groups ranges from 20 mm to 89 mm, the mean, median, range and 75th percentile of AGD values were determined for craniocaudal (CC) and mediolateral oblique (MLO) views. The differences in AGD values between FFDM and DBT were analyzed, and correlations among AGD and CBT, kVp, mAs and ESD were investigated.

Results: Across all CBT ranges, AGD values for DBT were (1.3±0.10) higher than those for FFDM. The DRLs at SQCCCRC range from 0.70 mGy to 2.55 mGy for FFDM and 0.94 mGy to 3.67 mGy for DBT, Fig. 1. The AGD highly showed correlation with kVp, mAs, ESD and CBT. A significant difference in the AGD value was noticed between FFDM and DBT acquisition in both CC and MLO projections (p < 0.005).

Conclusion: The study confirms that DBT generally results in higher AGD levels than FFDM across various CBT ranges, aligning with those established internationally. This research highlights the need for balancing radiation exposure with diagnostic accuracy in clinical decision-making, reinforcing DRLs as a benchmark for radiation safety in breast cancer screening practices.

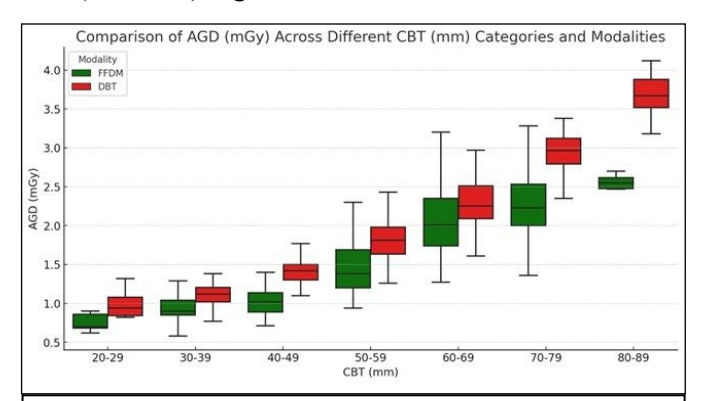


Fig.1: The AGD per woman for full-field digital mammography (FFDM) and digital breast tomosynthesis (DBT) at seven breast thickness groups

- Vañó, E., Miller, D. L., Martin, C. J., Rehani, M. M., Kang, K., Rosenstein, M., Ortiz-Lo'pez, P., Mattsson, S., Padovani, R., & Rogers, A. (2017). ICRP Publication 135: Diagnostic Reference Levels in Medical Imaging. Annals of the ICRP, 46(1), 1-144. https://doi.org/10.1177/0146645317717209.
- 2. Liu, Q., Suleiman, M. E., McEntee, M. F., & Soh, B. P. (2022). Diagnostic reference levels in digital mammography: a systematic review. Journal of Radiological Protection, 42(1). https://doi.org/10.1088/1361-6498/ac4214.

¹ Radiology and Nuclear Medicine Department, Sultan Qaboos Comprehensive Cancer Care and Research Centre (SQCCCRC), University Medical City, Muscat, Oman.

² Physics Department, College of Science, Sultan Oaboos University, Muscat, Oman.

³ Radiology and Molecular Imaging Department, College of Medicine, Sultan Qaboos University, Muscat, Oman.

EVALUATION OF MAMMOGRAPHY EQUIPMENT PERFORMANCE: A COMPARATIVE STUDY OF THREE AUTOMATIC PROTOCOLS

N. Hasan ¹, S. Alkhazzam ², M. Kharita ¹

¹ Salmaniya Medical Complex, Manama, Bahrain
 ² Occupational Health and Safety Department, Hamad Medical Corporation, Doha, Qatar

ABSTRACT

Background: Ensuring the performance of mammography units is essential to achieve optimal image quality and radiation dose outputs. The equipment's performance varies across different imaging protocols, each characterized by distinct exposure parameters that influence both image quality and radiation dose.

Objective: This paper aims to compare the differences in the performance of mammography unit implementing three available automatic protocols compared to the standard protocol using an automated quality control system with interactive Power Bi dashboard in order to enable healthcare professionals to adopt optimized practices in mammography imaging.

Methodology: This study compares three automatic imaging protocols in GE Sinographe Pristina mammography unit (STD-, STD+, and Implant) in reference to the standard protocol (STD), focusing on kV, mAs, image quality detectability d', and entrance skin dose ESD metrics. The clinical protocols were tested by the IAEA phantom and analyzed with the dedicated PyATIA software. The average of the above metrics was calculated for the three measurements of each protocol. and STD was used as a reference value to compare with STD- and STD+, Implant protocols.

Results: As shown in Fig.1, a reduction of mAs in the STD- protocol by 24% compared to mAs used in STD. Accordingly, ESD and d' reduced by 21 and 15%, respectively. In contrast, increasing the mAs in STD+ by 52% compared to STD increases the ESD and d' were increased by 50% and 16%, respectively. In addition, the increase in the mAs in the implant protocol by 18% compared to the STD increases the ESD by 12%; however, the d' is comparable to STD. Investigating the effect of adjusting the mAs in each protocol on the ESD and the d' compared to the STD protocol will provide insights into the effectiveness of each protocol.



Figure 1: The average values of kV, mAs, detectability at 0.3 mm and Entrance dose (mGy) of three images taken under each of the three automatic protocols (STD-, STD+, and Implant) compared with the standard protocol of the mammography imaging equipment

Conclusion: This study provides an understanding of mammography unit's performance through a comparative analysis of three automatic clinical protocols with the automatic standard one. The outcomes will afford insights for healthcare practitioners in mammography to optimize the equipment utilization.

- 1. International Atomic Energy Agency (IAEA). Implementation of a Remote and Automated Quality Control Programme for Radiography and Mammography Equipment. IAEA Human Health Series No. 39, IAEA; 2021.
- 2. Tsalafoutas IA,AlKhazzam S, Tsapaki V,AlNaemi H,Kharita MH. Digital radiography image quality evaluation using various phantoms and software. J Appl Clin Med Phys. 2022;23(12):e13823.

RADIATION DOSE MONITORING OF DENTAL RADIOLOGY WORKERS AT HAMAD MEDICAL CORPORATION: A FIVE-YEAR ANALYSIS (2020–2024)

A. Al Attar¹, S. Al Manea¹, C.M. De Castro¹, M.H. Kharita¹

ABSTRACT

Background: Occupational radiation exposure is a significant concern for healthcare professionals in radiological settings. Dental radiology workers, in particular, are frequently exposed to low-dose ionizing radiation due to the routine use of diagnostic imaging techniques. This study provides a comprehensive analysis of occupational radiation doses among dental radiology workers at Hamad Medical Corporation (HMC) hospitals in Qatar over five years (2020–2024). The aim is to evaluate compliance with international safety standards, identify long-term trends in radiation exposure, and establish an investigation dose level for this workforce.

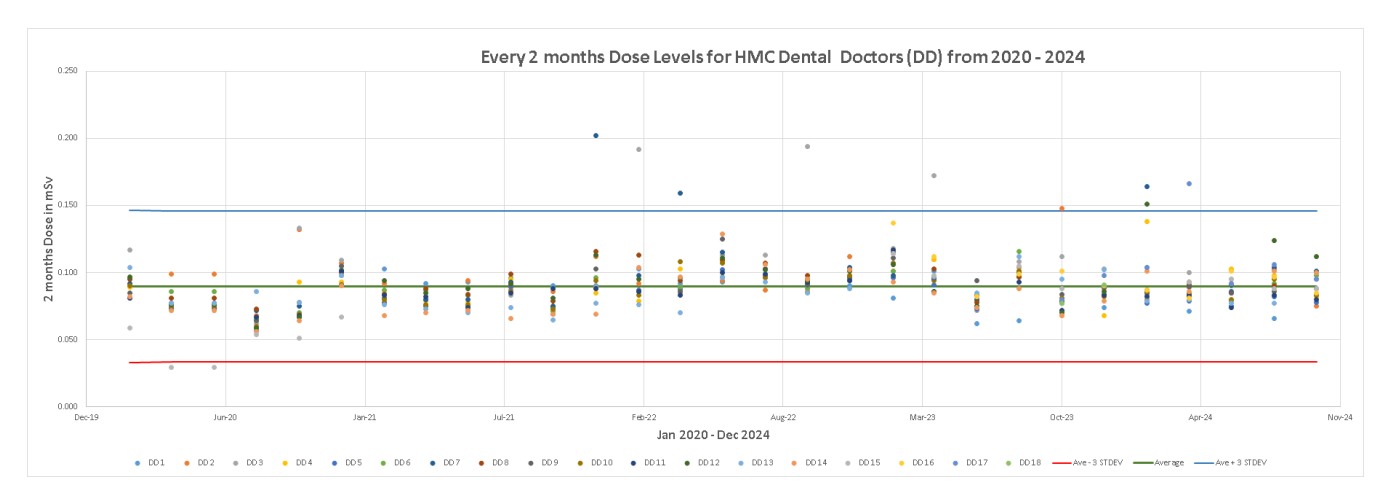
Objective: To establish a data-driven investigation dose level for dental radiology workers at HMC; Measure and analyze the effective doses received by dental radiology workers bi-monthly over five years (2020–2024); Compare exposure levels among three subgroups: dental assistants, dental technologists, and dental doctors; assess adherence to regulatory dose limits in Qatar.

Methodology: A total of 49 dental radiology workers from Rumailah Hospital, Al Khor Hospital, Al Wakra Hospital, Hazm Mebaireek General Hospital, and the Cuban Hospital were monitored. Participants were categorized into three subgroups: dental assistants, dental technologists, and dental doctors, based on their professional roles. Radiation doses were measured bi-monthly using Thermoluminescent Dosimeters (TLD-100, LiF: Mg, Ti), placed at chest level. Dosimeters were processed using the TLD Harshaw Reader 88000 at the Personal Dosimetry Laboratory under the Medical Physics section of HMC's Occupational Health and Safety Department. Statistical analysis was conducted to determine mean doses and standard deviations. A proposed investigation level was established based on the +3 standard deviation threshold.

Results: The bi-monthly average effective doses were consistent across the three subgroups: 0.089 mSv for dental assistants, 0.089 mSv for dental technicians, and 0.090 mSv for dental doctors. The analysis of the five-year dataset revealed that all measured doses fell well within safe levels, with 99% of values below the +3 standard deviation threshold. Based on these findings, an investigation dose level of 0.200 mSv was identified as the most appropriate threshold, aligning with the ALARA (As Low as Reasonably Achievable) principle.



¹ Occupational Health and Safety Department, Hamad Medical Corporation, Qatar.



Conclusion: This comprehensive five-year analysis highlights HMC's commitment to maintaining occupational radiation doses well within international safety standards. The introduction of an investigation dose level of 0.200 mSv reinforces HMC's leadership in radiation safety and exemplifies best practices in occupational radiation protection in healthcare settings.

- 1. https://www.iaea.org/resources/rpop/health-professionals/dentistry.
- 2. Recommendations of the International Commission on Radiological Protection (ICRP) (ICRP Publication, 1991) No: 60, 21.

EXTRACTION, SELECTION AND COMPARISON OF RADIOMIC FEATURES FROM CARDIAC REST AND STRESS SPECT/CT SCANS

R. AlMaashani¹, A. AlMaawali¹, A. AlMaimani², H. Nadeem², A. AlJabri², Y. Bouchareb³

¹Sultan Qaboos University, College of Science, Muscat, Oman.
²Sultan Qaboos University Hospital, Radiology and Molecular Imaging, Muscat, Oman.
³Sultan Qaboos University, College of Medicine and Health Sciences, Muscat, Oman.

ABSTRACT

Background: SPECT/CT is an imaging modality that has been used over few decades for the diagnosis and monitoring purposes of many cardiac diseases [1]. The application of artificial intelligence and radiomics has the potential to further enhance the detection, characterization, and prediction of diseases [2]. The extraction and selection of radiomics features that characterize cardiac SPECT/CT images could enhance further the diagnostic value of SPECT/CT imaging, help in reducing patient radiation doses, and improve clinical workflow.

Objective: The aim of this study was to investigate the potential of radiomics and artificial intelligence to characterize the differences in tissue patterns between rest and stress SPECT/CT scans, aiming to eliminate the need for rest scans by predicting results from stress scans alone.

Methodology: This research study included stress and rest cardiac SPECT/CT scans from 60 patients injected with Tc-99m Tetrofosmine (Myoview). The patients consist of 30 normal and 30 abnormal patients based on their ejection fraction. Patients with an ejection fraction greater than 50% were classified as normal while those with less than 40% were deemed abnormal. The cardiac SPECT/CT scans were selected from the local PACS at Sultan Qaboos University Hospital (SQUH) between January 1, 2023, and March 1, 2024. The DICOM images were uploaded to the 3D Slicer software for further processing. The 3D slicer segmentation tool was used to delineate the whole myocardium. Subsequently, features extraction from the segmented areas was performed using the SlicerRadiomics extension. For features selection, Principal Component Analysis (PCA) was utilized.

Results: A total of 107 radiomic features were extracted from the image series; falling into six categories: shape features, first order features, gray-level co-occurrence matrix (GLCM), gray level-run-length matrix (GLRLM), gray level-size-zone matrix (GLSZM), gray level-dependence matrix (GLDM), and neighboring gray-tone-difference matrix (NGTDM). PCA was used to reduce the feature set for the stress scans to 14, and 16 features for the rest scans, accounted for 78.7%, 73.4% of the total variance in the dataset, respectively.

Conclusion: The preliminary results from the study show that 14 and 16 features selected from stress and rest scans respectively describe the most pertinent features characterizing the myocardium tissue. Further analysis is needed to optimize feature selection by investigating other statistical methods that might provide better reduction for radiomic features.

- 1. Joel E, Bouchareb Y, et al. IEEE MIC (2014), Conference Record Paper. DOI:10.1109/NSSMIC.2014.7430861.
- 2. Bouchareb Y, AlSaadi A, Zabah J, et al. Diagnostics. 2024 Jul 4;14(13):1431. doi: 10.3390/diagnostics14131431.

CT-LESS PET ATTENUATION CORRECTION USING ARTIFICIAL INTELLIGENCE

A. Al Rahim Alaa¹, G. Amer², A. Souha², T. Tarraf^{2,3}, H. Rabih^{2,3}, M.H. Kharita², F. Hadi^{1,3}

ABSTRACT

Background: Positron Emission Tomography/Computed Tomography (PET/CT) integrates PET, providing functional imaging, with CT, offering anatomical details which enhances diagnostic precision. Nevertheless, challenges such as radiation exposure from CT scans and respiratory misalignments between PET and CT persist. Li et al. [1] introduced a deep learning-based method to eliminate CT radiation while preserving diagnostic accuracy. Similarly, Zhanli Hu et al. [2] addressed issues like attenuation correction and respiratory mismatches by employing deep learning models to generate Attenuation-Corrected PET (ACPET) from non-attenuation-corrected PET (NACPET). Despite these advancements, both studies relied on small datasets, limiting the robustness and clinical relevance of their results.

Objective: This project aims to develop a deep learning-driven approach utilizing a deep residual U-Net (DResUNET) model to generate Attenuation-Corrected PET (ACPET) images from Non-Attenuation-Corrected PET (NACPET) images.

Methodology: This study employed a 2D DResUNET [3] with an encoder-decoder architecture to generate attenuation-corrected (AC) PET images from non-attenuation-corrected (NAC) PET images. A dataset of 250 patients was used, with 175 allocated for training and 75 for validation. The model was trained for up to 100 iterations. To enhance learning and generalization, data augmentation techniques were applied, and the stochastic gradient descent (SGD) optimizer was utilized. The quality of the generated images was rigorously evaluated against reference images using quantitative metrics, including Mean Absolute Error (MAE) and Peak Signal-to-Noise Ratio (PSNR).

Results: In our study, the model achieved a PSNR of 52.95 ± 3.3 dB for synthetic ACPET, surpassing the PSNR of 40.841 ± 2.914 reported by Zhanli Hu et al. [2] and 34.03 ± 4.73 reported by Q. Li et al. [1], with a p-value of less than 0.05 based on Bland-Altman analysis. The model also achieved a mean absolute error (MAE) of 53.51 ± 20.60 for synthetic ACPET compared to the significantly higher MAE of 183.82 ± 117.5 for (NACPET).

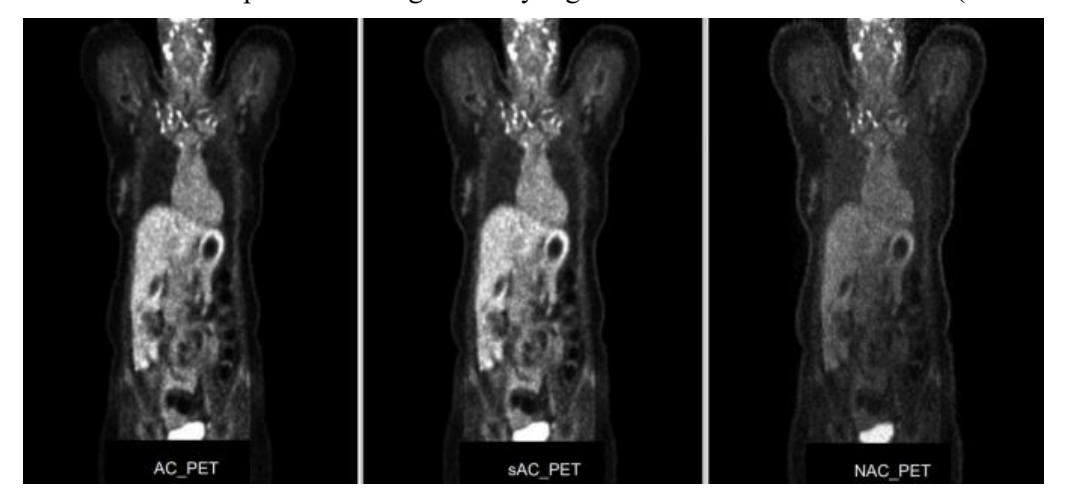


Fig. 1: Synthetic PET vs AC PET and NAC PET in DResUNET with 250 patients model training

Conclusion: The DResUNET framework successfully generated ACPET images from NACPET without relying on CT images. Future research will focus on generating CT images from the generated ACPET images.

¹ Occupational Health and Safety department, Hamad Medical Corporation, Qatar.

² Radiation Oncology Department, NCCCR, Hamad Medical Corporation, Qatar.

³ Weill Cornell Medicine, Qatar.

- 1. Q. Li *et al.*, "Eliminating CT radiation for clinical PET examination using deep learning," *Eur. J. Radiol.*, vol. 154, p. 110422, Sep. 2022, doi: 10.1016/j.ejrad.2022.110422.
- 2. Z. Hu *et al.*, "Obtaining PET/CT images from non-attenuation corrected PET images in a single PET system using Wasserstein generative adversarial networks," *Phys. Med. Biol.*, vol. 65, no. 21, p. 215010, Nov. 2020, doi: 10.1088/1361-6560/aba5e9.
- 3. H. Zunair and A. Ben Hamza, "Sharp U-Net: Depthwise convolutional network for biomedical image segmentation," *Comput. Biol. Med.*, vol. 136, p. 104699, Sep. 2021, doi: 10.1016/j.compbiomed.2021.104699.

A RETROSPECTIVE STUDY OF HIGH-DOSE-RATE BRACHYTHERAPY FOR CERVICAL CANCER TREATMENT USING 3D PRINTED APPLICATORS: A COMPARATIVE ANALYSIS WITH CONVENTIONAL APPLICATORS AT KFMC IN RIYADH

H.J. Alwadai¹, L.A. Al Mubarak ¹, M.A. Alqahtani ¹, T.A. Alrebdi¹

¹ Physics Department, Medical Physics program, College of Science, Princess Nourah Bint Abdulrahman University, Riyadh 11671, Saudi Arabia.

ABSTRACT

Background: Cervical cancer is a major health concern, with high mortality rates worldwide [1]. HDR brachytherapy is a crucial treatment modality, yet conventional applicators face challenges adapting to complex tumor shapes. Recent advancements in 3D printing technology enable the creation of customized applicator components, enhancing treatment precision and allowing for broader usability across multiple patients [2].

Objective: This study evaluates the efficacy and safety of 3D-printed applicators in HDR brachytherapy for cervical cancer, comparing their outcomes with conventional applicators to enhance precision and reduce complications.

Methodology: A total of 16 Stage II/III patients were treated at KFMC (2023-2024). Eight patients were treated with 3D Interstitial Ring and Tandem or 3D Multi-Channel Interstitial Cylinder, while the other eight received conventional applicators. Dosimetric evaluation ensured that 95% of the HRCTV was covered by the prescribed dose. Dose constraints for OARs were applied following ICRU Report 89 to minimize radiation toxicity. Statistical analysis was conducted using SPSS 26.0, with independent t-tests comparing dosimetric differences. Results were expressed as mean \pm SD and statistical significance was set at p < 0.05.

Results: For HRCTV, D95 achieved similar levels of dose coverage, with the mean for the conventional applicator at 99.3% and the 3D printed applicator at 99.7%, showing no statistically significant difference (P= 0.840). However, the 3D-printed applicator provided significant dose reductions to organs at risk (OARs), particularly the bladder and rectum. Significant reductions in bladder dose were observed at V25% (P= 0.005), V35% (P= 0.000), and V50% (P= 0.000), while rectal dose reductions were noted at V25% (P= 0.042), V35% (P= 0.023), and V50% (P= 0.012). These findings highlight the 3D-printed applicator's advantage in minimizing radiation exposure to OARs, thereby potentially reducing complications like urinary dysfunction and rectal toxicity. No significant differences were found for V15% in both organs (bladder: P= 0.192, rectum: P= 0.092).

Conclusion: 3D-printed applicators enhance treatment precision, ensuring safety and improved outcomes in HDR brachytherapy for cervical cancer. This innovative approach minimizes radiation-induced side effects and maximizes therapeutic benefits.

- 1. J. A. N. B. G. L. T. .. E. C. &. S. R. Song, "Elsevier," 2020. [Online]. Available: https://doi.org/10.1016/j.adro.2020.02.003.
- Z. z. g. Q. Z. G. H. L. J. Z. L. W. Y. Lu, "Research square," 19 4 2024. [Online]. Available: https://doi.org/10.21203/rs.3.rs-4247955/v1.

IDENTIFYING HUMAN ERRORS IN AUTOMATED RADIOGRAPHIC QUALITY CONTROL SYSTEMS USING ADVANCED POWER BUSINESS INTELLIGENCE

S. Alkhazzam¹, and M.H. Kharita¹

ABSTRACT

Background: Digital radiography is a cornerstone of modern medical diagnosis, routinely employed to detect diseases and fractures. Given its critical role, rigorous quality control is imperative. Traditionally, this task is conducted annually by medical physicists. To support this process and enhance its effectiveness, the International Atomic Energy Agency (IAEA) has developed an automated and remote solution. This innovative approach leverages a straightforward phantom and the open-source software PyATIA to evaluate the image quality of radiographic systems.

Objective: To investigate the influence of human errors on radiographic image quality metrics across various exposure conditions using an automated quality control system with interactive Power Bi dashboard.

Methodology: Fourteen different scenarios were designed for possible situations that a technician might encounter while doing the test of the IAEA Phantom, and the results were compared with the assumed baseline value of the correct setup.

Results: The results presented in the figure below illustrate the following effects: increasing the SID from 110 cm to 120 cm enhances detectability by 13% and raises the exposure index by 16%. Reducing the kV from 81 to 70 kV improves detectability by 8% but decreases the exposure index by 26%. Rotating the phantom by 30 degrees does not affect the detectability index (d') or exposure index (EI). Selecting the right and left AEC chambers results in a slight increase in d' (8%) and EI (24%). Using added filters (0.1 or 0.2 mm Cu) causes a slight change in d' and EI (5%). Choosing Speed 200 significantly impacts d' (43%) and EI (108%). Increasing contrast by +2 raises d' by 27% and EI by 63%. Selecting a small FS has minimal effect on d' and EI.

No.	SID	FOV [cm x cm]	kV	AEC	Cropping	Position	Filters	Added Filters	Speed	FS size	Contrast
01	110	35 X 35	81	С	Cropping	Aligned	2 mm Cu	No	S400	Large	0
02	110	35 X 35	81	С	No Cropping	Aligned	2 mm Cu	No	S400	Large	0
03	90	35 X 35	81	С	Cropping	Aligned	2 mm Cu	No	S400	Large	0
04	120	35 X 35	81	С	Cropping	Aligned	2 mm Cu	No	S400	Large	0
05	110	28 X 28	81	С	Cropping	Aligned	2 mm Cu	No	S400	Large	0
06	110	28 X 28	81	С	No Cropping	Aligned	2 mm Cu	No	S400	Large	0
07	110	35 X 35	70	С	Cropping	Aligned	2 mm Cu	No	S400	Large	0
08	110	35 X 35	81	R+L	Cropping	Aligned	2 mm Cu	No	S400	Large	0
09	110	35 X 35	81	С	Cropping	Rotate 30°	2 mm Cu	No	S400	Large	0
10	110	35 X 35	81	С	Cropping	Cu shift up toward AEC	2 mm Cu	No	S400	Large	0
11	110	35 X 35	81	С	Cropping	Aligned	2 mm Cu	0.1 Cu	S400	Large	0
12	110	35 X 35	81	С	Cropping	Aligned	2 mm Cu	0.2 Cu	S400	Large	0
13	110	35 X 35	81	С	Cropping	Aligned	2 mm Cu	No	S200	Large	0
14	110	35 X 35	81	С	Cropping	Aligned	2 mm Cu	No	S400	Large	+2
15	110	35 X 35	81	С	Cropping	Aligned	2 mm Cu	No	S400	small	0



¹ Occupational Health and Safety Department, Hamad Medical Corporation, Qatar.

Conclusion: By implementing a Python-based Automated Image Analysis Tool with a dedicated dashboard, we can effectively isolate human errors resulting from test setup mistakes. This allows us to filter these errors from the results, enabling accurate monitoring of radiography system performance and predicting potential future deterioration.

- 1. International Atomic Energy Agency (IAEA). Implementation of a Remote and Automated Quality Control Programme for Radiography and Mammography Equipment. IAEA Human Health Series No. 39, IAEA; 2021.
- 2. Tsalafoutas IA,AlKhazzam S, Tsapaki V,AlNaemi H,Kharita MH. Digital radiography image quality evaluation using various phantoms and software. J Appl Clin Med Phys. 2022;23(12):e13823.
- 3. Tsalafoutas IA, AlKhazzam S, Tsapaki V, Kharita MH. Automatic image quality evaluation in digital radiography using for-processing and for-presentation images. J Appl Clin Med Phys. 2024 Apr;25(4):e14285. doi: 10.1002/acm2.14285. Epub 2024 Feb 5. PMID: 38317593; PMCID: PMC11005988.

PERFORMANCE OF THE SHIELDING OF RADIATION PROTECTION GLOVES USING HAND ANTHROPOMORPHIC PHANTOM

S. Alkhazzam¹, and M.H. Kharita¹

¹ Occupational Health and Safety Department, Hamad Medical Corporation, Qatar.

ABSTRACT

Background: Interventional radiology procedures involving X-ray imaging pose a significant radiation risk to healthcare workers, particularly their hands. To mitigate this risk, lead gloves are widely employed. However, these protective measures can inadvertently increase radiation exposure to both patients and operators by interfering with the primary radiation beam and consequently amplifying scattered radiation.

Objective: To assess the radiation protection effectiveness of the SensiCare PI gloves and the impact of hand placement in the primary radiation field on increased exposure.

Methodology: Materials used for the study include Dosimeter (Raysafe X2) with stand 30 cm + attenuator 2 mm Cu, Rad-Fluoroscopy unit (tube over table)- SIEMENS Luminos dRF, radiation field 30×30 cm, Anthropomorphic phantom (Hand), SensiCare PI Shield Radiation Protection Gloves. The radiation output of different energies (60, 81, 100, and 121 kV) was measured at a distance of 75 cm from the focal spot of the x-ray tube, using 2 mm of copper (simulating the attenuation of a human body). The measurement setup is shown in Figure 1.

Results: The results are presented in Table 1: radiation dose, dose rate, HVL, and total radiation. The glove was placed on an anthropomorphic phantom of a hand and the dosimeter was placed between the hand and the glove to measure the radiation attenuation of the glove as shown in Figure 2. The radiation air kerma measurements were recorded for different energies (60,81,100, and 121 kV), and the results are presented in Table 1 (with and without gloves). The radiation attenuation in the glove was calculated from the ratio of the radiation dose with the glove over the radiation dose without glove. The results are shown in Table 2.





Figure 1. radiation measurement of 75% of the gloves within the radiation field

Table 1.	Table 1. The radiation output of the radiographic mode at 75 cm from the focal spot at different kVs									
1.17	m A a	*** ***		mGy	n	Gy/s		HVL		TF
kV	mAs	ms	w/o	w/Gloves	w/o	w/Gloves	w/o	w/Gloves	w/o	w/Gloves
60	10	100	537	195	5.33	1.94	2.4	3.5	3.3	6.8
81	10	100	1025	470	10.21	4.68	3.2	4.8	3.2	6.8
100	5	100	755	389	7.57	3.90	4.0	5.6	3.2	6.9
121	5	100	1059	596	10.63	6.00	4.7	6.4	3.3	7.0

Table 2. The attenuation values using the gloves at different	nt kVs (efficiency of radiation shielding)
kV	Attenuation ratio
60	64%
81	54%
100	48%
121	44%

Conclusion: These gloves provide partial protection against ionizing radiation, as they attenuate the radiation to the hands of the radiation workers by ~60-40% for the voltage range from 60 to 120 kV, respectively. This confirms the specifications provided by the vendor.

THE INFLUENCE OF VMAT AND TREATMENT SITE ON RADIATION USE FACTOR DETERMINATION

M. Alfishawy¹, N. Babu¹, I. Al Amri¹, M. Gurumani¹, Z. Al Mandhari¹

¹ Sultan Qaboos Comprehensive Cancer Center (SQCCC)/Radiation oncology, Muscat, Oman.

ABSTRACT

Background: The use factor (U) quantifies the fraction of beam-on time during which the primary radiation beam is directed toward a specific barrier. With the growing adoption of advanced radiotherapy techniques such as Volumetric Modulated Arc Therapy (VMAT), U may vary depending on treatment technique and site.

Objective: This study evaluates and compares the use factors for two TrueBeam machines treating different schemes of treatment sites with different fractions of technique type.

Methodology: Data from two identical TrueBeam linear accelerators, Machine A and Machine B, were analyzed over 30 months. Machine A predominantly treated head and neck, chest, and breast cases, while Machine B focused on pelvic, palliative, total body irradiation, and breast cases. Beam-on time data were extracted from the ARIA reporting system and analyzed across four gantry angle ranges: 315°–45°, 45°–135°, 135°–225°, and 225°–315°, corresponding to the floor, right wall, ceiling, and left wall barriers, respectively.

Results: The proportion of VMAT treatments was 33% for Machine A and 63% for Machine B. Use factors for Machine A were distributed as follows: floor (26%), right wall (21%), ceiling (31%), and left wall (22%). For Machine B, the use factors were floor (15%), right wall (8%), ceiling (69%), and left wall (8%). Radiation shielding calculations for Machine B were updated based on the revised use factors, confirming compliance with safety standards.

Conclusion: Advanced radiotherapy techniques and treatment site distributions influence use factor calculations. This study highlights the importance of incorporating clinical data into use factor assessments to ensure adherence to radiation safety standards.

- 1. d'Errico F. Structural shielding design and evaluation for megavoltage x- and gamma-ray radiotherapy facilities: NCRP Report No. 151 Published. Radiat Prot Dosimetry 2006;121(3):342-3.
- 2. Rodgers JE. Radiation therapy vault shielding calculational methods when IMRT and TBI procedures contribute. J Appl Clin Med Phys 2001;2(3):157-64.

ENHANCING PATIENT SAFETY THROUGH RADIOGRAPH REJECTION ANALYSIS: INSIGHTS FROM A DIAGNOSTIC IMAGING DEPARTMENT AUDIT

M. Yaseen¹, T. Nishtar¹, R. Ajaj², A. Ali¹

Department of Radiology, Lady Reading Hospital, Peshawar, Pakistan.
 Environmental Health & Safety Department, Abu Dhabi University, Abu Dhabi, UAE.

ABSTRACT

Background: Medical Imaging is one of the most important modalities despite being associated with some radiation exposure to patients. One of the main goals of quality assurance program in diagnostic imaging is to produce consistently high-quality radiographs with minimum exposure to patients creating images of sufficient quality for the clinical task, not of unnecessarily high quality resulting in high patient doses due to repetition. Thus, rejection analysis is an integral part of the QA program to evaluate image quality discouraging unnecessary repetitions.

Objective: Assessment of actual radiograph rejection was the primary goal of this audit in the diagnostic imaging facility of a public sector.

Methodology: Total of 47,300 radiographic examinations were analyzed retrospectively for the rejected radiographs and their causes at the department of Radiology, Lady Reading Hospital from Jan - Dec 2022.

Results: Of the total, 5203 procedures were repeated resulting in 11% rejection with 46.1% rejection observed in male and 53.9% in female respectively. Artifacts (26.2%) was the prime cause of rejection followed by motion (18.8%), positioning (14%), improper collimation (11.7%), exposure errors (8.4 %), wrong labeling (6.6%), machine faults (5.7 %), detector errors (4.5%), PACS issues (2.5 %) and re-request from referring physician (1.6%) as highlighted in figure. The highest rejection with respect to anatomical body parts was observed in chest radiography (29.9%), followed by extremities (28.8%), spine (11.4%), KUB (9.9%), skull (8.4%), abdomen (5.5%), pelvis (4.4%), and neck (1.7%) respectively.

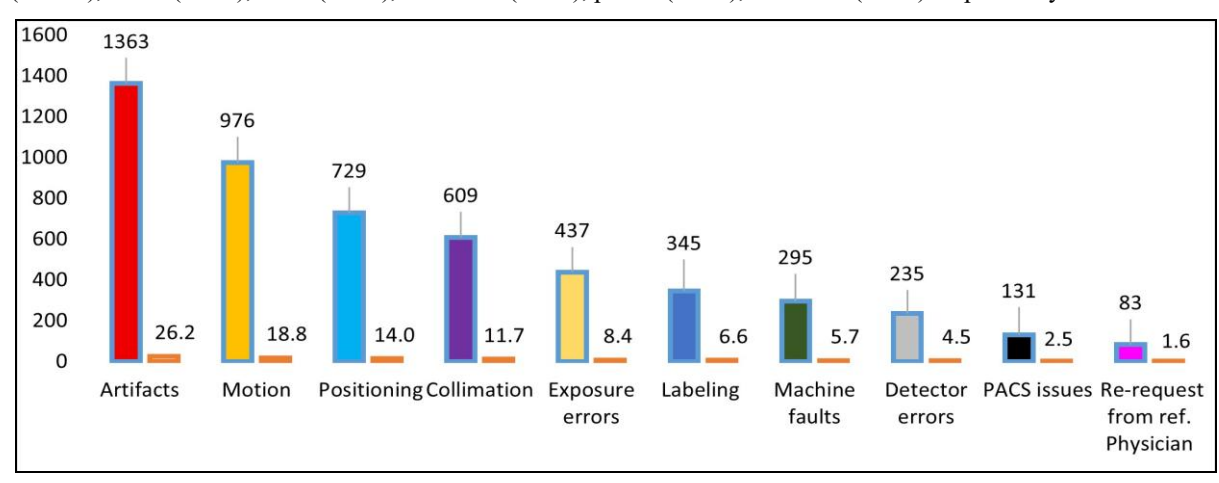


Figure 1: Rejected radiographs with respect to causes of rejection

Conclusion: Radiograph rejection has reduced considerably but still remains common problem within the facility due to many contributing factors. Implementation of rejection analysis as integral part of quality assurance program along with focusing on staff-centered skill & knowledge upliftment training programs can result in significant reduction in percentage of digital radiograph rejection.

- Ali RT. Assessment of X-Ray Rejected Films and Image Quality in Diagnostic Radiology Departments of Teaching Hospitals in Iraq. Research Square. 2023: 1-12.
- 2. Alahmadi OS, Alrehaili AA, Gameraddin MB. Evaluation of reject analysis of chest radiographs in diagnostic radiology. Am .J. Diagn. Imaging. 2019. 5(1):4-8.

LUNG CANCER SEGMENTATION WITH A U-NET ARCHITECTURE FOR IMPROVED TUMOR DIAGNOSIS, TREATMENT PLANNING, AND RADIOTHERAPY

A. Ayadi^{1,2}, B.O. Mdimagh³, C.I. Hammami^{1,2}

 Tunisian Center for Nuclear Sciences and Technology, Technopark Sidi Thabet, Tunisia.
 Research Laboratory on Energy and Matter for Nuclear Science Development (LR16CNSTN02), Ministry of Higher Education and Research, Tunisia.

³ UTM, Higher Institute for Medical Technologies of Tunis.

ABSTRACT

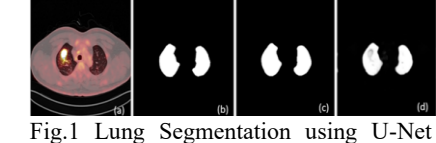
Background: Lung cancer remains the leading cause of cancer-related mortality globally, highlighting the urgent need for effective early detection methods to improve patient outcomes [1]. Accurate segmentation of lung tumors in medical imaging plays a critical role in diagnosis, treatment planning, and radiotherapy. Medical physicists rely on precise delineation of tumor boundaries to ensure optimal radiation dose delivery while minimizing exposure to healthy tissues. This underscores the importance of developing robust segmentation models for lung cancer.

Objective: The primary objective of this research is to enhance the performance of the U-Net model [2] for lung cancer segmentation by implementing a modified architecture. This study aims to evaluate the effectiveness of the enhanced U-Net model in accurately segmenting lung tumors and lung tissue in CT-PET images.

Methodology: The proposed method utilizes a modified U-Net architecture that incorporates four convolutional blocks, allowing for deeper feature extraction compared to the standard three. The system was validated using the Lung-PET-CT-Dx dataset [3]. Performance metrics, such as the Dice coefficient, Jaccard index, F1-score, accuracy, precision, sensitivity, and loss values using both Binary Cross-Entropy (BCE) and Dice loss functions, were calculated to assess the model's effectiveness.

Results: For the lung segmentation task, the U-Net achieved a BCE loss of 0.96, a Dice coefficient of 0.93, a Jaccard index of 0.96, an F1-score of 0.99, an accuracy of 0.96, a precision of 0.96, and a sensitivity of 0.99. For tumor segmentation, the performance metrics were a BCE loss of 0.74, a Dice coefficient of 0.59, a Jaccard index of 0.74, an F1-score of 0.99, an accuracy of 0.80, and a precision of 0.69. The segmentation of lung and tumor is illustrated in Figure 1 and 2, respectively.

Conclusion: This study demonstrates the potential of the enhanced U-Net model for automating lung cancer segmentation in CT-PET images, crucial for improving diagnostic accuracy. However, further refinement is needed, particularly in tumor segmentation, to minimize misclassifications and enhance performance.



model: (a) Input Image; (b) Mask; (c) Prediction Mask with Dice; (d) Prediction Mask with BCE.

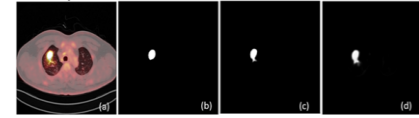


Fig.2 Tumor Segmentation using U-Net model: (a) Input Image; (b) Mask; (c) Prediction Mask with Dice; (d) Prediction Mask with BCE.

- International Agency for Research on Cancer (IARC). (2024). New report on global cancer burden in 2022 by world region and human development level.
- 2. Ronneberger, O., Fischer, P., & Brox, T. (2015). U-Net: Convolutional Networks for Biomedical Image Segmentation. In: Lecture Notes in Computer Science, pp. 234-241. https://doi.org/10.1007/978-3-319-24574-4_28.
- 3. The Cancer Imaging Archive (TCIA). LUNG-PET-CT-DX The Cancer Imaging Archive (TCIA). The Cancer Imaging Archive (TCIA). 2024. https://www.cancerimagingarchive.net/collection/lung-pet-ct-dx/

BREAST SIZE-BASED TYPICAL VALUES IN MAMMOGRAPHY: A CASE STUDY IN SRI LANKA

K. Somarathne^{1,2}, G. Muthumali², K. Dhanaraj², S. Welarathna^{1,2}, B. Hewavithana³, S. Sarasanandarajah^{4,5,6}, S. Velautham²

Postgraduate Institute of Science, University of Peradeniya, Peradeniya, Sri Lanka.
 Department of Physics, University of Peradeniya, Peradeniya, Sri Lanka
 Department of Radiology, University of Peradeniya, Peradeniya, Sri Lanka.
 School of Health and Biomedical Sciences, RMIT University, Melbourne, Australia
 Department of Physical Sciences, Peter MacCallum Cancer Center, Australia
 Department of Medical Physics, Bharathiar University, Coimbatore, India

ABSTRACT

Background: Mammography is a vital X-ray imaging modality for the early detection of breast cancer and related conditions. Given the radiosensitivity of glandular breast tissue, it is crucial to adhere to the "as low as reasonably practicable" (ALARP) principle to ensure maximum patient safety¹.

Objective: This study aimed to develop breast-size-based typical values for entrance surface dose (ESD) in digital mammography examinations conducted at a tertiary care hospital in Sri Lanka.

Methodology: The retrospective study included 761 adult patients (3,044 mammograms) aged over 18 years who underwent diagnostic mammography between January 2022 and December 2023. Data extracted from the digital mammography system (Hologic Lorad Selenia) included patient age, compressed breast thickness (CBT), kilovoltage peak (kVp), milliampere-seconds (mAs), and ESD. Patients were categorized into three groups based on CBT: Group 1 (10–39 mm), Group 2 (40–69 mm), and Group 3 (70–89 mm). Statistical analysis determined typical values for each breast size group, using the median ESD as recommended by ICRP Publication 135².

Results: The typical values obtained for the entire range of CBT were 4.70 mGy for the CC view (CBT range: 12–84 mm) and 7.02 mGy for the MLO view (CBT range: 14–88 mm).

	Table - Typical valu	ies for different CBT group	os .
CBT range (mm)	Mammographic	Number of	Typical value
	Projection	mammograms	(mGy)
10 - 39	CC	126	3.7
	MLO	24	4.03
40 - 69	CC	417	5.56
	MLO	440	7.80
70 - 89	CC	18	11.10
	MLO	90	12 13

Breast-size-based typical values reduced the ESD for Group 1, with 20.85% the CC for view and 42.59% for the MLO view. A positive correlation between CBT and ESD was observed, consistent with existing literature.

Conclusion: This study highlights the significance of breast-size-based typical values for optimizing radiation doses and enhancing patient safety. Such an approach can help reduce patient radiation exposure and serve as a model for dose optimization in healthcare settings in Sri Lanka.

- 1. Breast cancer. Accessed January 16, 2024. Https://www.who.int/news-room/fact-sheets/detail/breast-cancer.
- 2. Clement CH, ed. Diagnostic Reference Levels in Medical Imaging. SAGE; 2017...

RADIATION DOSE MONITORING OF NUCLEAR MEDICINE DEPARTMENT STAFF: A FIVE-YEAR ANALYSIS (2020-2024)

A. Ghujeh¹, H. Fayad¹, A. Abd Al Rahim¹, A. AlAttar¹, M. Kharita¹

¹ Occupational Health and Safety Department, Hamad Medical Corporation, Qatar

ABSTRACT

Background: Occupational radiation exposure is a critical concern for healthcare professionals in nuclear medicine, particularly those handling radiopharmaceuticals. This study analyzes radiation doses recorded over five years (2020–2024) among Nuclear Medicine Department staff to assess exposure trends and the impact of expanding radiotherapy procedures, including Lu-177 PSMA and Y-90 synovectomy.

Objective: The study seeks to - Evaluate whether the investigation levels need adjustment to account for the increased use of radioisotopes in the department; Calculate the average quarterly doses for each group and assess trends in their exposure levels; Identify factors contributing to dose variations, with a particular focus on Cyclotron staff and Technologists.

Methodology: Radiation exposure for Nuclear Medicine and Molecular Imaging (NMMI) staff members was monitored every two months using Thermoluminescence Dosimeters (TLDs) worn at chest level. Staff were categorized into four groups: Physicians, Technologists, Nurses, and Cyclotron staff. TLDs were processed at the Personal Dosimetry Laboratory using the TLD Harshaw Reader 8800. Monitored doses averages were calculated, and statistical analyses identified trends. Investigation reports were triggered when doses exceeded the investigation level of 0.7 mSv per monitoring period of 2 months.

Results: Over the past five years, average doses were 0.101 mSv (Physicians), 0.249 mSv (Nurses), 0.329 mSv (Technologists), and 0.193 mSv (Cyclotron staff), with mean + 3 SD values of 0.943 mSv and 0.885 mSv for Technologists and Cyclotron staff, respectively. In the last two years, averages increased to 0.106 mSv, 0.262 mSv, 0.339 mSv, and 0.445 mSv, with mean + 3 SD rising to 0.980 mSv and 1.246 mSv for Technologists and Cyclotron staff.

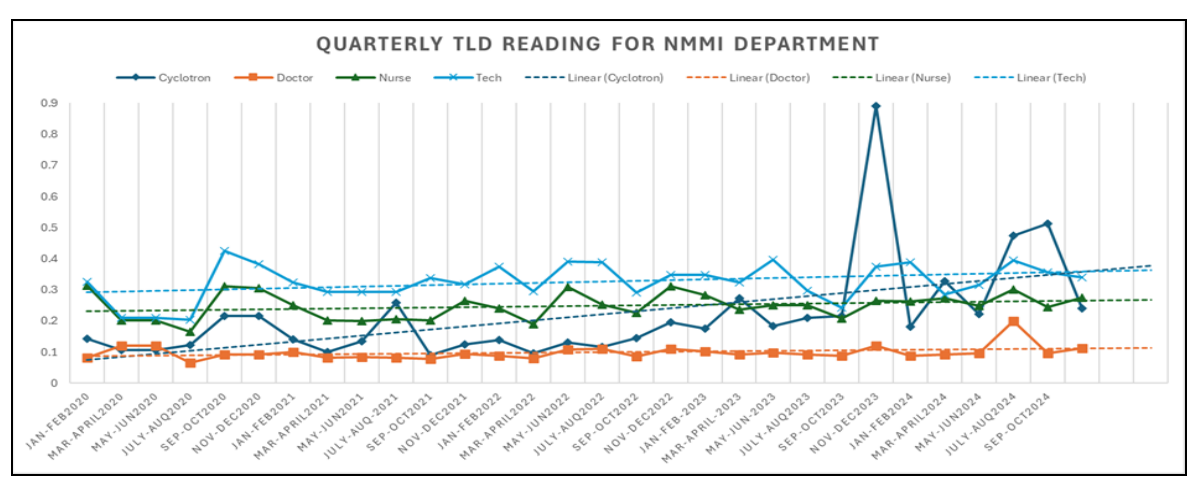


Figure 1: Average dose for each subgroup- on two monthly monitoring period from 2020 - 2024

Conclusion: The findings highlight the impact of radiotherapy expansion on occupational exposure, particularly for Cyclotron staff and Technologists. Adjusting the investigation level to 1 mSv per two months is recommended to accommodate the evolving workload in nuclear medicine especially for the Cyclotron staff. Continuous monitoring and updated safety protocols remain essential for maintaining staff safety.

THE IMPACT OF THE HALF-LIFE OF FLUORINE-18 DEPENDING ON THE PURITY LEVEL OF HEAVY WATER ON THE IMAGE QUALITY OF PET-SCAN IMAGING

H.H. Alabedi^{1,2}, M.A. Alrawi², N.M. Ali³, M.S. Almusawi⁴, R. Ahmad³

¹ Surgery Department, College of Medicine, Baghdad University, Baghdad, Iraq.
² Cyclotron Unit, Warith International Cancer Institute, Karbala, Iraq.

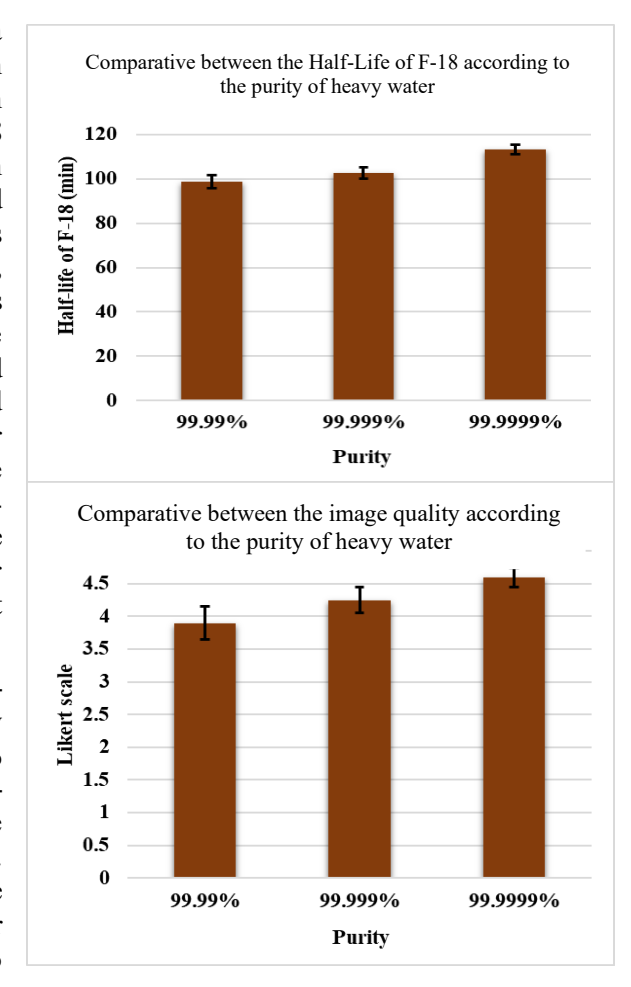
ABSTRACT

Background: Positron Emission Tomography (PET) modality is mainly used in detecting and staging tumors. Many factors influence the image quality of PET scans, but most importantly, the radiopharmaceuticals used. The fluorine-18 is a commonly used isotope due to its short half-life and high efficiency of positron emission. The properties of heavy water (O_2H_{18}) for isotope play a significant role in the radiobiological process and can alter with radiation produced by F-18 and hence of PET scanning quality.

Objective: This study aimed to investigate the impact of the half-life of Fluorine-18 on the image quality of PET-scan depending on the percentage for the heavy water purity level of O_2H_{18} (99.999)%, O_2H_{18} (99.9999)%, and O_2H_{18} (99.999)%.

Methodology: This is a prospective study with a convenience sampling technique performed at Warith International Cancer Institute (WICI), Karbala, Iraq, between May and October 2025. A total of 108 samples of Florine-18 were used in this study, divided into three types depending on the purity of the heavy water (O₂H₁₈ or oxygen-18 enriched water); each type contains 36 samples. These percentages were prepared under specific conditions, which are 99.99%, 99.999%, and 99.9999%. The preparation of Fluorine-18 was done in a cyclotron and performed by the irradiation of the deuteron to an O₂H₁₈. The half-life was tracked and recorded during the production each time. The half-life was measured using a spectrometer at specific time intervals after production to measure the decay rate. The images were acquired by PET/CT (Biograph Horizon PET/CT scanner 64 slices, Siemens Healthcare, Munich, Germany). The image quality was assessed by three nuclear medicine specialists for each patient, and an average was calculated using a Likert scale. The statistical analysis was performed by SPSS 28.

Results: The study shows that the mean half-life of Fluorine-18 prepared by O_2H_{18} with heavy water with 99.99% purity was 98.66 ± 2.99 min, while those prepared with 99.999% purity were 102.66 ± 2.48 min. Furthermore, the mean half-life for 99.9999% purity was 113.33 ± 1.98 min. The difference between these half-lives was high, with p ≤ 0.0001 . The quality of images was found to be significantly (p-value of 0.003) higher (4.6 ± 0.15) at Fluorine-18 with heavy water purity of 99.9999%, followed by 4.25 ± 0.2 for 99.999%



³ Center for Diagnostic, Therapeutic and Investigative Studies (CODTIS), Faculty of Health Sciences, Universiti Kebangsaan Malaysia, Kuala Lumpur, Malaysia.

⁴ College of Medical Sciences, Jabir Ibn Hayyan Medical University, Kufa, Iraq

purity and 3.9 ± 0.25 for 99.99% purity, respectively. The confidential interval (CI) of 95% was approximately 103.6 to 106.1 minutes. It was found that there is a strong positive correlation between image quality and purity of heavy water.

Conclusion: It was found that the best image quality resulted from the higher purity of heavy water (99.9999%) and longer half-life. The study shows that a longer half-life produces a better image quality for PET scans.

- 1. Katal S, Eibschutz LS, Saboury B, Gholamrezanezhad A, Alavi A. Advantages and Applications of Total-Body PET Scanning. Vol. 12, Diagnostics. 2022.
- 2. Mostafapour S, Greuter M, van Snick JH, Brouwers AH, Dierckx RAJO, van Sluis J, et al. Ultra-low dose CT scanning for PET/CT. Med Phys. 2024;51(1).
- 3. Khalil MM. Basic science of PET imaging. Basic Science of PET Imaging. 2016.
- 4. Jacobson O, Kiesewetter DO, Chen X. Fluorine-18 radiochemistry, labeling strategies and synthetic routes. Vol. 26, Bioconjugate Chemistry, 2015.
- 5. Lin M, Shon IH, Lin P. Positron emission tomography: Current status and future challenges. Vol. 40, Internal Medicine Journal. 2010.

REGRESSION-BASED MACHINE LEARNING FOR DOSE PREDICTION AND OPTIMIZATION IN CHEST X-RAY EXAMINATIONS

S. Welarathna^{1,2,3}, S. Viswakula⁴, V. Sivakumar², S. Sarasanandarajah^{5,6,7}

Postgraduate Institute of Science, University of Peradeniya, Peradeniya, Sri Lanka.
 Department of Physics, University of Peradeniya, Peradeniya, Sri Lanka.
 Faculty of Graduate Studies, University of Sri Jayewardenepura, Nugegoda, Sri Lanka.
 Department of Statistics, University of Colombo, Colombo, Sri Lanka
 School of Health and Biomedical Sciences, RMIT University, Melbourne, Australia
 Department of Physical Sciences, Peter MacCallum Cancer Center, Melbourne, Australia
 Department of Medical Physics, Bharathiar University, Coimbatore, India

ABSTRACT

Background: Chest X-ray examinations are among the most frequently performed radiographic examinations worldwide. The variations in manual exposure settings in clinical practice often result in significant differences in patient doses, underscoring the need for effective dose optimization strategies to enhance patient protection.

Objective: This study aimed to develop and evaluate regression-based machine learning (ML) models for predicting and optimizing patient dose in chest X-ray examinations.

Methodology: Data from 1,060 chest posteroanterior examinations were analyzed, with predictors including BMI, kilovoltage peak, tube current-exposure time product, and X-ray system type. The kerma-area product was used as the target dose metric. Outliers were handled using the Local Outlier Factor method. Categorical variables were processed using one-hot encoding. Multicollinearity was tested and statistically significant variables were selected. Min-Max normalization and Yeo-Johnson transformations were applied to address skewness in both predictor and target variables. Twenty-five regression models were evaluated using PyCaret's automated ML framework in Python, with an 80:20 training-testing split. Hyperparameter tuning was performed using Optuna-based random search. Model performance was assessed using 10-fold cross-validation, with evaluation metrics including coefficient of determination (R²), mean absolute error (MAE), and root mean squared error (RMSE).

Results: The Gradient Boosting Regressor (GBR) demonstrated the highest predictive performance, achieving an R^2 of 0.7357 (± 0.0820), MAE of 0.0428 (± 0.0033), and RMSE of 0.0605 (± 0.0056). Hyperparameter tuning further refined model performance by optimizing key parameters (n_estimators, learning_rate, max_depth, min_samples_split, min_samples_leaf, subsample, and max_features). The tuned model achieved a slightly improved predictive accuracy, with an R^2 of 0.7366 (± 0.0771), MAE of 0.0428 (± 0.0028), and RMSE of 0.0605 (± 0.0051). Learning curve and residual analyses confirmed the GBR model's enhanced generalization capability and reduced prediction errors compared to other regression models.

Table 1 Evaluation of top 5 models in terms of performance metrics

	2	F		
Model	\mathbb{R}^2	MAE	RMSE	
Gradient Boosting Regressor	0.7357	0.0428	0.0605	
CatBoost Regressor	0.6921	0.0459	0.0653	
Random Forest Regressor	0.6801	0.0465	0.0675	
Light Gradient Boosting Machine	0.6771	0.0476	0.0671	
K Neighbours Regressor	0.6625	0.0484	0.0686	

Conclusion: The GBR model enables patient-specific dose prediction, allowing radiographers to proactively adjust exposure parameters and maintain doses within diagnostic reference levels without compromising image quality. The integration of ML predictive models into clinical workflows could facilitate personalized dose optimization, standardize practices, reduce overexposure, and enhance patient protection. Future research should explore deep learning models trained on larger datasets and incorporate image quality metrics for further dose optimization.

- 1. Garcia-Sanchez et al. Machine learning techniques applied to dose prediction in computed tomography tests. Sensors (Basel). 2019;19(23). doi:10.3390/s19235116.
- 2. Python (v. 3.11.11), NumPy (v. 1.26.4), Pandas (v. 2.2.2), Matplotlib (v. 3.10.0), Seaborn (v. 0.13.2), SciPy (v. 1.13.1), scikit-learn (v. 1.5.2), PyCaret (v. 3.3.2).

EVALUATION OF NOISE-EQUIVALENT COUNTS AND SIGNAL-TO-NOISE RATIO IN (18)F-FDG PET/CT RECONSTRUCTION METHODS: A COMPARATIVE STUDY OF TOF, TOF+PSF, AND PSF-ONLY TECHNIQUES

S. Al-Rawahi¹, S. Kheruka¹, N. Al-Maymani¹, N. Al-Makhmari¹, H. Al-Saidi¹, S. Al-Rashdi¹, A. Al-Balushi¹, K. Al-Riyami¹, R. Al-Sukaiti¹

ABSTRACT

Background & Objective: This study investigates the impact of point-spread function (PSF) and time-of-flight (TOF) reconstruction techniques on (18)F-FDG PET/CT imaging, focusing on noise-equivalent counts (NEC). It aims to evaluate the correlation between NEC and signal-to-noise ratio (SNR) for three reconstruction methods: TOF, PSF, and TOF+PSF.

Methodology: Thirty patients underwent (18)F-FDG PET/CT scans for cancer evaluation, excluding cases with liver metastases to ensure uniformity in liver assessments. Images were reconstructed using three distinct methods: (1) TOF, which enhances image quality by improving localization of detected photons; (2) PSF, which models the physical point-spread function to correct spatial resolution degradation; and (3) TOF+PSF, which combines the benefits of TOF and PSF for optimized image quality. For each reconstruction method, the SNR was calculated by drawing three volumes of interest (VOIs) on the liver. The NEC in the liver was estimated from the sinogram header data. Spearman's rank correlation coefficient was employed to analyze the relationship between NEC and SNR for each reconstruction method.

Results: TOF+PSF reconstruction achieved excellent SNR, producing superior image quality with enhanced contrast and reduced noise. The PSF-only reconstruction demonstrated a significant increase in SNR due to its ability to correct spatial resolution degradation, resulting in images with reduced noise. TOF reconstruction provided moderate improvements, benefiting from enhanced photon localization. No significant correlation was observed between NEC and SNR across all reconstruction methods, indicating that NEC alone does not adequately predict image quality in reconstructed PET/CT images.

Conclusion: The combined TOF+PSF method offers the most significant enhancement in PET/CT image quality, making it a promising choice for clinical imaging. The PSF-only method also improves image quality by effectively reducing noise and enhancing spatial resolution. The absence of a correlation between NEC and SNR underscores the need for multifaceted image quality assessment metrics beyond NEC in PET/CT imaging.

¹ Sultan Qaboos Comprehensive Cancer Care and Research Center, Dept. of Radiology and Nuclear Medicine, Muscat, Oman.

ASSESSMENT OF OCCUPATIONAL DOSES TO RADIATION WORKERS AT LADY READING HOSPITAL, PESHAWAR, PAKISTAN (2017-2023)

A. Ali¹, M. Yaseen¹, R. Ajaj², T. Nishtar¹, K. Rehman³

¹ Department of Radiology, Lady Reading Hospital, Peshawar, Pakistan.
 ² Environmental Health & Safety Department, Abu Dhabi University, Abu Dhabi, UAE
 ³ Health Physics Division, Pakistan Institute of Nuclear Science and Technology, Islamabad, Pakistan.

ABSTRACT

Background: Ionizing radiation has revolutionized the modern era of medicine with high degree of precision and accuracy, but their detrimental effects cannot be underestimated. Therefore, their judicious use is necessary to ensure safety of patients along with enforcement of personnel dose monitoring for occupational staff to ensure their safety.

Objective: The aim of this study was to assess the occupational doses to various groups of workers during the past seven (07) years (2017-2023) and to check the compliance of the ICRP annual dose limit of 20 mSv.

Methodology: A retrospective analysis of dose records of 12012 film badge dosimeters used in various modalities were carried during the study period. The distribution of workers, annual average effective doses, annual average collective effective doses, minimum and maximum individual doses & average annual effective doses in various dose intervals were analyzed for the above stated period.

Results: The annual effective dose in Diagnostic Radiology, Cath Lab, Gastroenterology, Neurosurgery, Orthopedic & Urology were 0.74-1.75, 1.04-2.06, 0.43-1.13, 0.37-1.13, 0.35-1.14 & 0.5-1.65 mSv respectively. The min. & max. Annual effective doses measured were 0.1 & 8.8, 02 & 9.9, 0.2 & 2, 0.3 & 2.8, 0.3 & 2.5, 0.3 & 3.5 mSv respectively in DR, CCL, Gastro, NS, Ortho. & Urology. The majority of workers (85%) received doses in the interval 1-5.99 mSv while (12%) staff received doses within the range of minimum detectable limit (MDL) -0.99 mSv while around 03% of staff received doses above the action level 06 mSv. The annual average effective doses (AAED) are depicted in the figure.

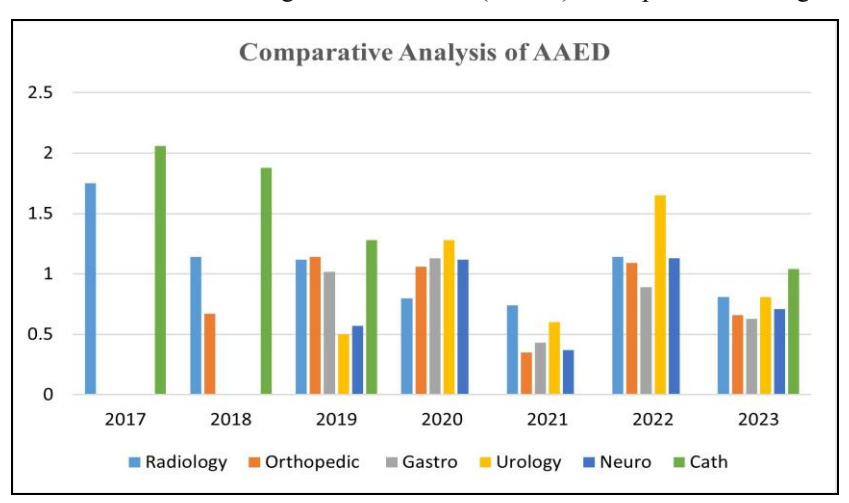


Fig: Comparative analysis of average annual effective doses (AAED) of radiation workers

Conclusion: The annual effective doses received by various groups of occupational staff were less than annual dose limits which reflect strict adherence to radiation protection and practical implementation of ALARA principle.

- T. Nishtar, M. Yaseen, A.Ali. (2018). Radiation awareness amongst radiation workers in diagnostic radiology department of a public sector hospital in khyberpakhtunkhwa; PJR 28(1): 40-44.
- International Commission on Radiological Protection. 1990 Recommendations of the international commission on radiological protection, ICRP Publication 60. Oxford: Pergamon Press; 1991.

A DOSIMETRIC ANALYSIS OF ORGANS AT RISK FOR PATIENTS TREATED WITH 177 LU-PSMA

A. Al-Balushi¹, N. Al-Maymany¹, S. Kheruka¹, H. Al-Saidi¹, K. Al-Riyami¹

¹ Sultan Qaboos Comprehensive Cancer Care and Research Center / Radiology and Nuclear Medicine Department, University Medical City, Muscat, Oman

ABSTRACT

Background: Lutetium-177 Prostate-Specific Membrane Antigen (¹⁷⁷Lu-PSMA) therapy is a targeted radionuclide therapy used for the treatment of metastatic castration-resistant prostate cancer (mCRPC). Excessive radiation to kidneys and salivary glands can lead to nephrotoxicity or xerostomia necessitating careful dose monitoring.

Objective: This study aims to measure the absorbed doses to the kidneys and the salivary glands for the first cycle of therapy and correlate them with observed side effects.

Methodology: The study involved 3 patients treated with ¹⁷⁷Lu-PSMA at SQCCCRC, with the post-therapy imaging done at two time points, 2-4 hours and 24-48 hours. All patients in our study completed six cycles of therapy except for one patient who stopped after cycle 3 due to disease progression. Post-therapy imaging was performed using two methods: (1) tomographic (SPECT/CT) only and (2) a hybrid method combining a series of planar images with a single delayed SPECT/CT image.

Results: The mean absorbed doses for the kidneys and the salivary glands were 0.583 ± 0.117 Gy/GBq (range: 0.36-0.76 Gy/GBq) and 0.057 ± 0.042 Gy/GBq (range: 0.014-0.139 Gy/GBq), respectively as shown in Figure 1. No decline in renal function or toxicities were observed. However, xerostomia was reported in one patient following the third cycle; this patient received an accumulated dose of 3.42 Gy by the 3rd cycle, which was the highest recorded in our study group even from the patients who completed 6 cycles.



Fig. 1 Mean Absorbed Dose per Administered Activity

Conclusion: Our findings show a correlation between the incidence of xerostomia and the absorbed dose to the salivary glands with no evident correlation between kidney absorbed dose and renal toxicities. The tolerance limits for absorbed radiation doses to the kidneys and salivary glands in radiopharmaceutical therapies remain inconsistently defined, highlighting the importance of performing dosimetry to explore these thresholds and tailor patient care. Additionally, with more patient data, we could potentially identify subgroups that are particularly sensitive to radiation dosages, which would further refine our dosimetric techniques and improve personalized treatment plans.

INFLUENCE OF PATIENT BODY SURFACE AREA ON THE SELF-ATTENUATION FACTOR OF THE PATIENT BODY IN ¹⁸F-FDG PET-CT SCANS: A PILOT STUDY

Y. Lahfi¹, N. Alkerdi¹, T. Ayach¹

¹ Protection and Safety Department, Atomic Energy Commission of Syria, Syrian Arab Republic

ABSTRACT

Background: During hybrid PET-CT imaging, close contact with patients impacts radiation doses received by staff and the public. To measure how the radiation absorption and scattering is affected by a patient's body after radioactive dose administration, the patient self-attenuation factor (PAF) was introduced. The Body Surface Area (BSA) may be used to assess the patient's radiation exposure to maintain levels within safe thresholds based on body size.

Objective: The purpose is to determine how the PAF and BSA correlate during ¹⁸F-FDG PET-CT examinations.

Methodology: Fifteen patients administered with ¹⁸F-FDG for PET-CT scans were monitored. Their age, height, weight, and administered radioactivity were recorded, and their BMI and BSA were calculated. The radiation dose rate from unshielded ¹⁸F-FDG syringe just before injection at 1 meter was measured. The external radiation dose rate from the standing patient immediately post dose administration, to avoid the radioactivity decay correction, at a distance of 1 meter was measured at three different levels: head, thorax and knee and their average value was calculated. The PAF was calculated as the ratio between the external radiation dose rate measured from the patient with that measured from the unshielded ¹⁸F-FDG syringe. A calibrated radiation monitor TRACERCO T202 (UK) was used to measure the expected dose rate in the study.

Results: The average BMI and BSA of the patients' sample were 27.88±6.29 kg m⁻² and 1.85±0.23 respectively, and the administered 18F-FDG radioactivity was from 333 to 444 MBq. The average normalized external dose rates from the patient and the unshielded ¹⁸F-FDG syringe were 0.10±0.02 and 0.17±0.01 μSv h⁻¹ MBq⁻¹ respectively, and the average of the calculated PAF was 0.55±0.11. The relationship between the PAF and the BSA was investigated by calculating the Pearson correlation coefficient R² value of the linear regression test. Its value of 0.75 indicates a good association between them (Fig. 1).

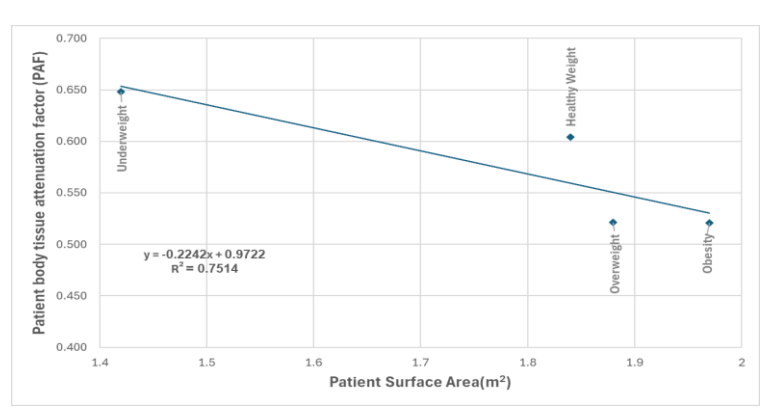


Fig. 1 The relationship between BSA and the PAF in the four BMI classification groups: Underweight, Healthy Weight, Overweight, Obesity

Conclusion: The established correlation between PAF and BSA can be used to approximate the radiation dose received from the patient, especially during close contact with medical staff. This will positively impact the optimization of staff radiation protection during PET-CT scans.

References:

1. Khaled Soliman, Ahmed Alenezi, Measurements of dose rate constant corrected for self attenuation from patients injected with 18F (FDG), Physica Medica, Volume 32, Supplement 3, 2016, Page 285.

OPTIMAL HOME ISOLATION DURATION FOR DIFFERENTIATED THYROID CARCINOMA PATIENTS TREATED WITH HIGH-DOSE I-131

H. Al Saidi¹, B. Al Abri², A. Al Bulushi¹, A.Z. Al Kindi², S. Al Rashdi¹, N. Al Maymani¹, N. Al Makhmari¹, S. Kheruka¹

ABSTRACT

Background: Radioiodine therapy using Iodine-131 has been a cornerstone in the treatment of differentiated thyroid cancer since the 1940s. Its efficacy in eliminating residual thyroid tissue and metastatic thyroid cancer has been well-documented. However, the optimal post I-131 therapy isolation duration for patients with differentiated thyroid carcinoma is widely debated.

Objective: This study aims to determine the most effective home isolation period for these patients following a two-day hospital stay, focusing on protecting the public from radiation risks and enhancing patients' well-being, who often experience anxiety and unpredictability.

Methodology: The total estimated dose equivalent for those in contact with patients was determined by considering external dose rates and whole-body retention assessments. Dose rates were measured using a solid-state detector at the patient's umbilicus and neck level. The retained activity estimate included both direct gamma photon counting and indirect activity estimation via dose rates.

Results: For an administered activity of 1.1 GBq, patients required three days of sleeping separately and avoiding close contact with pregnant women and children, with no precautions necessary for adult family members. For higher administered activities (3.7 GBq, 5.5 GBq, and 7.4 GBq), five days of sleeping apart and avoiding close contact with pregnant women and children were required, plus two days of avoiding close contact with adults. Based on the total effective dose equivalent threshold of less than 5 mSv, all patients could be released from the hospital without isolation after a two-day stay.

Conclusion: The optimal patients' isolation duration was evaluated based on estimated public dose equivalent. The study provides significant data for the management of patients treated with high-dose I-131, enhancing patient care and public safety.

- 1. International Atomic Energy Agency (IAEA). Radiation Protection and Safety in Medical Uses of Ionizing Radiation: IAEA Safety Guide No. SSG-46. Vienna: IAEA; 2018. Section 2.49.
- 2. International Atomic Energy Agency (IAEA). Release of Patients After Radionuclide Therapy: Safety Reports Series No. 63. With contributions from the ICRP. Vienna: IAEA; 2009. Annex II, Section 11-1, p. 48.
- 3. United States Nuclear Regulatory Commission (US NRC). Release of Patients Administered Radioactive Materials: Regulatory Guide 8.39. Washington, DC: US Nuclear Regulatory Commission.
- 4. Lee, J.H. and Park, S.G., 2010. Estimation of the release time from isolation for patients with differentiated thyroid cancer treated with high-dose I-131. *Nuclear Medicine and Molecular Imaging*, 44, pp.241–245.

¹ Radiology and Nuclear Medicine Department, Sultan Qaboos Comprehensive Cancer Care and Research Centre, Muscat, Oman
² College of Science, Sultan Qaboos University, Muscat, Oman

REDUCING RADIATION DOSE IN PET/CT IMAGING WITHOUT COMPROMISING QUALITY

M. Al-Abedi¹, N. Alsaedi¹, N. Ibrahim¹, D. Abualsaud², H. Aljamei², A. Alumair², E. Alwuhaib², A. Albuali²

 $^{\rm 1}$ Medical Physics Department, King Fahad Specialist Hospital-Dammam, Saudi Arabia $^{\rm 2}$ Nuclear Medicine Department, King Fahad Specialist Hospital-Dammam (KFSHD), Saudi Arabia

ABSTRACT

Background: Since 2014, the standard practice for administering F18-FDG doses in PET/CT scans at KFSHD has consistently been set at 10 mCi (for a 70 kg adult), despite advancements in imaging technology. In 2023, an opportunity was identified to optimize the existing PET/CT system to reduce radiation doses, aligning with ALARA (As Low as Reasonably Achievable) principles to minimize radiation exposure for patients and staff while maintaining diagnostic quality. However, concerns regarding potential impacts on image quality and lesion detectability have delayed the implementation of a reduced-dose protocol.

Objective: To reduce the F18-FDG standard dose for PET/CT scans by 30% (from 10 mCi to 7 mCi) without compromising the diagnostic quality of imaging.

Methodology: A total of 100 patients underwent PET/CT scans with optimized F18-FDG doses. Data from 37 patients were analyzed by nuclear medicine physicians who were blinded to the administered doses. Image quality was evaluated using a 4-point scale. Mean standardized uptake values (SUV) and standard deviations (SD) were recorded from uniform liver regions, excluding patients with hepatic pathologies. Initially, the dose reduction protocol targeted lymphoma patients, with subsequent expansion to follow-ups based on positive feedback from nuclear medicine physicians.

Results: Over 95% of scans with an optimized dose were rated as 'Excellent' or 'Good,' demonstrating diagnostic reliability. Less than 5% were categorized as 'Poor but interpretable,' with no cases marked as 'Non-diagnostic. Mean SUV across evaluations averaged 1.8 with a standard deviation of 0.2-0.23, confirming consistency with the 10 mCi protocol. Follow-up scans showed high correlation with baseline images, ensuring diagnostic continuity. Artifacts and noise were minimal, without diagnostic impact. Average doses administered were 6.93 mCi (range: 5.0–8.9 mCi), adjusted based on body weight. Fig. 1 shows a 37-year-old female with a history of double malignancy post-therapy. The top row presents a study performed in May 2023 with 7.7 mCi F18-FDG, while the bottom row presents a study performed in January 2023 with 10.3 mCi F18-FDG for the same patient. No significant change in resolution, quality, or FDG biodistribution between the two studies.

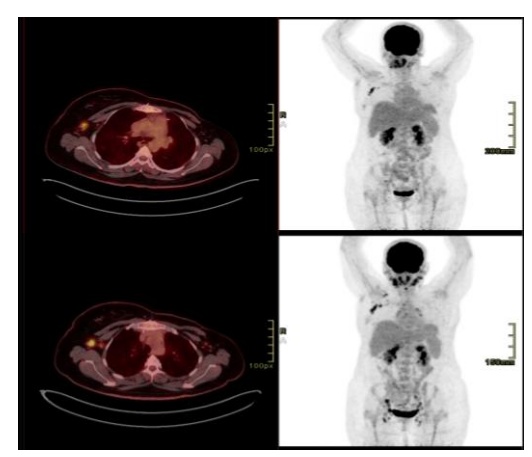


Fig. 1 Comparative F18-FDG PET/CT scans at different dose levels in a post-therapy patient.

Conclusion: This project demonstrates the feasibility of reducing F18-FDG doses in PET/CT imaging. The implementation of a 7 mCi protocol represents a substantial advancement in patient care and staff safety. Future steps include continuous monitoring and further optimization based on clinical outcomes.

INVESTIGATION OF ALERT LEVELS IN INTERVENTIONAL RADIOLOGY PROCEDURES PERFORMED IN HAMAD MEDICAL CORPORATION

A. Aly¹, A. Barah², I. Tsalafoutas¹, H. Al Hammar², A. Omar², M. H. Kharita¹

¹ Hamad Medical Corporation, Medical Physics section, OHS Department, Qatar ² Hamad Medical Corporation, Clinical Imaging Department, Qatar

ABSTRACT

Background: The use of ionizing radiation for medical purposes has greatly contributed to the improvement of healthcare services regarding the diagnosis and treatment of numerous pathological conditions. During the last decades radiology has been greatly developed and has been used by various medical specialties as a useful tool in image guided surgical procedures. More importantly, a new branch of radiology has been established which combines diagnosis and treatment on the spot, commonly referred to as interventional radiology, since radiologists do not only diagnose but also treat patients. Interventional radiology procedures (IR) have replaced many surgical procedures since they are equally effective but also minimally invasive, something which minimizes complications but also reduces hospitalization time and the associated costs.

Objective: The main objective is to determine the frequency of occurrence of tissue reactions in patients from different types of Fluro-Guided Interventional (FGI) procedures reference to the recommendation addressed by IAEA.

Methodology: The study was performed in a dedicated IR facility, located in a large general hospital of HMC. This facility is comprised of two interventional suites, equipped with two modern identical IR systems.

Results: HMC adopted trigger levels for PKA, $K_{a,r}$ and FT will result in PSD values of 0.83, 2.49 and 0.67 Gy when the adopted trigger lever for PSD is set to 1 Gy, whereas the respective IAEA trigger levels will result in PSD values of 2.07, 4.15 and 0.96 Gy when the adopted trigger lever for PSD is set to 3 Gy. Thus, the fitting results of this dataset suggest that the trigger level for PKA and even more the trigger level for FT are set too low with respect to the PSD, whereas the $K_{a,r}$ trigger levels are set too high, since the PSD versus $K_{a,r}$ line slope is about 0.8, much larger than the 0.6 (=3/5) assumed by the IAEA trigger levels.

Conclusion: Patient radiation protection is not a luxury but a necessity and should be considered more like a culture where the principles are always practiced by all the personnel involved in IR procedures, in all IR suites of an institution and not occasionally applied in the context of a project or by only some of the personnel and in some IR suites only.

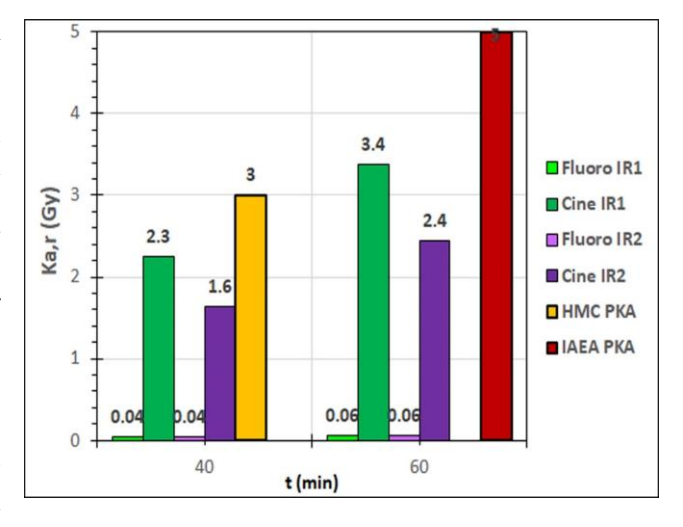


Figure 1: P_{KA} for 40 and 60 min of fluoro and cine acquisitions for the two IR systems (IR1 and IR2), compared to the respective HMC and IAEA trigger level values (FOV=Zoom1, 2 mm Cu).

- 1. National Council on Radiation Protection and Measurements. Radiation dose management for fluoroscopically guided interventional medical procedures. Report 168. Bethesda, MD: National Council on Radiation Protection and Measurements; 2010.
- 2. Stecker MS, Balter S, Towbin RB, Miller DL, Vañó E, Bartal G, et al. Guidelines for patient radiation dose management. J Vasc Interv Radiol 2009; 20(7 Suppl): S263–73. doi: https://doi.org/10.1016/j.jvir.2009.04.037.

INDOOR RADON MEASUREMENT IN SOME HAMAD MEDICAL CORPORATION HOSPITALS: BASE LINE DATA

A. Aly¹, R. Shwikani², O. Bobes¹, M. Al Homaid¹, C. Mark¹, A. AlAttar¹, R. Abdul Rahman¹, H. Gaili¹, D. Lemma¹, N. Sahid¹, S.M. Al Manea¹, M.H. Kharita¹

¹ Hamad Medical Corporation, Occupational Health & Safety Department, Qatar ²Atomic Energy Commission, protection and Safety Department, Syria

ABSTRACT

Background: Radon is a naturally occurring decay product of the elements uranium and thorium. When it escapes from rocks and soils it is harmlessly dispersed unless contained by structures. When radon gas is inhaled by occupants it is largely exhaled leaving only a very small fraction to decay and irradiate tissue because it is radiologically not very active, having a half-life of 4 days. Exposure due to radon might occur in all types of workplaces and facilities, ranging from conventional offices, hospitals, naturally occurring radioactive material processing industries, underground facilities, and nuclear fuel cycle facilities. The health risk associated with radon has grown over the last decades. In the past, the health effect of radon was the frequent lung disease (lung cancer) incidence among underground miners. However, nowadays attention is paid to radon both at workplaces and homes.

Objective: The objective of this study is to understand the radon levels present in Hamad Medical Corporation (HMC) hospitals and to establishing a sustainable, Qatar-based radon monitoring and mitigation system that protects the health of both healthcare workers.

Methodology: Two methods were used for radon level measurements: - (1) Passive method: 10 radon chambers (CR39 detectors) were prepared and used for passive measurements at some accessible workplaces in the basements at some HMC hospitals kept for 30 days; (2) Active method: Using AlphaGUARD radon measurements equipment located in medical physics section. AlphaGUARD is used for occupational radon measurement at HMC workplaces. This equipment is very good to give instant radon concentration at any place. The AlphaGUARD was kept for 2 hours in these places.

Results: These results indicated that the average concentration of radon during the monitoring period was $66 \pm 25 \text{ Bq.m}^{-3}$ which is higher than the average expected (25 Bq.m⁻³) and lower the action level (200 Bq.m⁻³). However, it is recommended to set up a radon monitoring program covering occupied workplaces at the basements and ground floors in all HMC buildings. In addition, it is also recommended to study the avarage radon cencentrations in Qatar dwallings, using long term measurements (CR-39). This could be done by setting a monitoring programme covery different areas in Qatar counties, and foucasing on the basments and ground levels. The measurements of active methods using AlphaGUARD equipments in different HMC places shows low radon concentrations than the passive methods, this might be due to the high sensitivity of CR-39 and the duration of the measurements.

Table 1 Comparing the radon levels using active and passive measurements method in some HMC places

Location	CR 39 Detector	AlphaGUARD
A1	76 ± 4	5.3±4.7
A2	96 ± 3	3.2±1.6
A3	52 ± 3	3.3±1.5
A4	Detector's Background	9.6 ± 8.6
A5	83 ± 5	16.5 ± 8.0
A6	100 ± 5	6.5±1.8
A7	30 ± 3	4.7±2.2
A8	32 ± 2	21.4 ± 9.6
A9	58 ± 3	7.2±2.5
Background	Detector's Background	-



Figure 1: Selected areas for radon concentration in different HMC places using active and passive methods, Area (A1-A9)

Conclusion: These are the instructions for preparing papers for the Medical Physics International Journal. English is the official language of the Journal. Read the instructions in this template paper carefully before proceeding with your paper.

- 1. Statistical Estimate of Radon Concentration from Passive and Active Detectors in Doha, Kassim Mwitondi 1,*, Ibrahim Al Sadig 2, Rifaat Hassona 2, Charles Taylor 3 and Adil Yousef 4. http://www.mdpi.com/journal/data, Data 2018.
- 2. Indoor air quality in naturally ventilated italian classrooms. Atmosphere ,Fuoco, F.C.; Stabile, L.; Buonanno, G.; Trassiera, C.V.; Massimo, A.; Russi, A.; Mazaheri, M.; Morawska, L.; Andrade, A. 2015, 6, 1652–1675.

ESTABLISHMENT OF LOCAL DIAGNOSTIC REFERENCE LEVELS (LDRL'S) FOR FLUORO GUIDED INTERVENTIONAL RADIOLOGY PROCEDURES: SINGLE FACILITY STUDY AT LADY READING HOSPITAL, PESHAWAR PAKISTAN

A. Ali¹, M. Yaseen¹, S. Burki¹, R. Ajaj²

¹ Department of Radiology, Lady Reading Hospital, Peshawar Pakistan ² Environmental Health & Safety Department, Abu Dhabi University, UAE

ABSTRACT

Background: The extended use of Interventional procedures in diagnostic Radiology has increased the potential threat of high radiation doses to both patients and occupational staff involved in these procedures. Therefore, establishment and implementation of Local Diagnostic Reference Levels (DRLs) is of utmost importance in restricting the occupational doses as well in patient dose optimization obtaining optimum image quality.

Objective: The purpose of study was to establish DRLs for Fluoro-Guided Interventional Radiology Procedures (FGIPs) at Lady Reading Hospital, Peshawar enhancing safe radiation practice by setting specific benchmarks in terms of lower occupational doses, patient dose optimization & image quality obtaining better therapeutic outcomes.

Methodology: The study focused on various FGIPs conducted in the interventional Radiology section compiling data including Dose Area Product, Air kerma rate, fluoroscopy time, frame rate, kilovoltage & (mAs). The data pertained to adult patients of age > 50 years having weights ranging between 50-80kg. DRLs were set as the third (03rd) quartile of DAP values & fluoroscopy time.

Results: The DRL values in-terms of DAP (Gy*cm²) and fluoroscopy time (min) at 75th percentile for the types of procedures carried out during the course of study were: Trans-Arterial Chemo-Embolization (TACE): DAP: 103.4 Gy*cm², FT: 12.2 min, Percutaneous Transhepatic Biliary Duct (PTBD): DAP: 13.1 Gy*cm², FT: 4.3 min, Biopsies: DAP: 52.2 Gy*cm², FT: 0.6 min, Perma-Catheter Placement: DAP: 5.4 Gy*cm², FT: 2.2 min, Cholangiogram: 3.5 DAP: Gy*cm², FT: 1.3 min, Digital Subtraction Angiography (DSA): DAP: 50.5 Gy*cm², FT: 11.3 min, Venoplasty: DAP: 73.2 Gy*cm², FT: 13.8 min, Drainage placement: DAP: 37.5 Gy*cm², FT: 1.2 min & DJ Stenting: DAP: 52.2 Gy*cm², FT: 26.8 min illustrated in Figure.

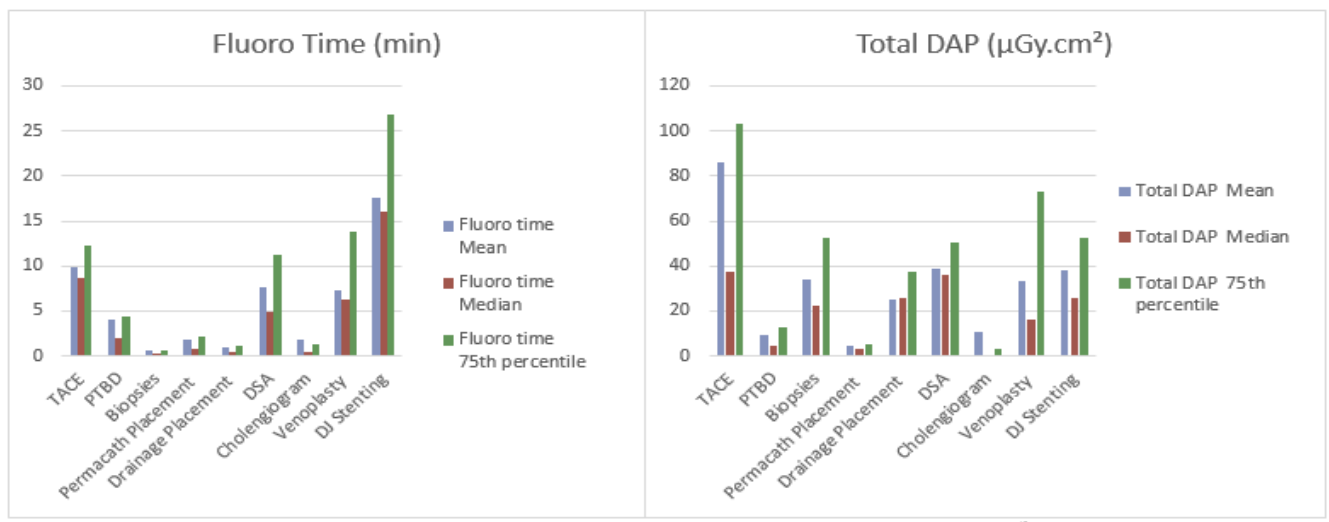


Fig: The DRL values in-terms of DAP (Gy*cm²) and fluoroscopy time (min) at 75th percentile for the types of procedures carried during the course of study

Conclusion: The DRLs in FGIPs at LRH are consistent with international studies, ensuring radiation doses within limits highlighting safe radiation practices. This study will open new horizons for the more effective use of resources in achieving ALARA goals in FGIR settings.

- Mahesh M. (2012). Radiation Dose Management for Fluoroscopically Guided Interventional Medical Procedures. Med Phys. 39(9), 5789–90.
- 2. Padovani, R., Foti, C. and Malisan, M. R. (2001). Staff Dosimetry Protocols in interventional Radiology, Radiation Protection Dosimetry. 94(1-2), 09.

COMPARATIVE ANALYSIS OF 3DCRT AND IMRT TREATING PLAN TECHNIQUES IN RADIOTHERAPY FOR CERVICAL CANCER IN GHANA: A CASE STUDY OF KOMFO ANOKYE TEACHING HOSPITAL (KATH)

H. Juma¹, E. Addison^{1,2}, F. Hasford^{1,3}

Department of Medical Physics, School of Nuclear and allied Sciences, University of Ghana, Accra, Ghana
 Oncology Directorate, Komfo Anokye Teaching Hospital, Kumasi, Ghana
 Radiological and Medical Sciences Research Institute, Ghana Atomic Energy Commission, Accra, Ghana

ABSTRACT

Background & Objective: The study was conducted to propose an evidence-based treatment protocol for IMRT personalized to patient needs at KATH.

Methodology: The 3D-CRT technique was designed using a single isocenter, field-in-field technique with the standard four-field box technique to optimize dose delivery while minimizing exposure to OARs. The IMRT technique utilized a single isocenter with seven fields and dynamic multi-leaf collimators to enhance PTV coverage and minimize OAR exposure.

Results: Results showed significant differences in the maximum dose (D_{max}) delivered to the PTV and OARs, with IMRT offering better sparing. In cervical cancer, the mean D_{max} to the bladder was lower for IMRT (46.588±1.693 Gy) compared to 3D-CRT (47.739±0.915 Gy), with a p-value of 0.028. In prostate cancer, the mean D_{max} to the rectum was lower in IMRT (75.831±1.166 Gy) than in 3D-CRT (77.322±1.354 Gy), with a p-value of 0.004. IMRT improved dose distribution, reducing radiation to OARs and the risk of secondary cancers. For cervical cancer, the mean homogeneity index (HI) was 1.052±0.032 for 3D-CRT and 1.079±0.020 for IMRT (p=0.007). The conformity index (CI) for both techniques was similar (3D-CRT: 0.98±0.01, IMRT: 0.98±0.01, p=0.786). In prostate cancer, the HI was 1.080±0.161 for 3D-CRT and 1.062±0.017 for IMRT (p=0.687), and the CI was comparable (3D-CRT: 0.983±0.010, IMRT: 0.966±0.013, p=0.529). Both techniques showed similar dose homogeneity and conformity.

Conclusion: This study supports the implementation of IMRT as the standard treatment modality at KATH due to its normal tissue-sparing capabilities.

- 1. Drokow, E. K., Liu, Z., Wang, T., Su, J., Yuan, W., Shi, F., Li, Y., Sasu, E., & Xu, L. (2020). Dosimetric Comparison and Clinical Toxicity in Cervical Cancer Patients Treated with Intensity- Modulated and Three-Dimensional Conformal Radiotherapy: Real-World Data. *Cancer Studies and Therapeutics*, 5(4), 1–7. https://doi.org/10.31038/cst.2020541.
- 2. Ekici, K., Kuloglu, M., Ata, A. O., Atahan, O., & Tiryakioglu, O. (2022). A Dosimetric Comparison of 7 Field IMRT, 9 Field IMRT, VMAT and 3-D Conformal Radiotherapy for the Treatment of Localized Intermediate Risk Prostate Cancer. *UHOD Uluslararasi Hematoloji-Onkoloji Dergisi*, 32(3), 133–140. https://doi.org/10.4999/uhod.226166.

DEVELOPING AN INDEPENDENT MU CHECK SCRIPT FOR CYBERKNIFE PLANS

M. Najem¹

¹ Radiation Oncology Department, King Saud University Medical City, Riyadh, Saudi Arabia

ABSTRACT

Background: The verification of monitor unit (MU) calculations is a critical component of quality assurance (QA) in radiotherapy, as highlighted by international guidelines [1]. However, access to independent MU calculation software is limited in many radiotherapy centers.

Objective: This study aims to develop an independent MU calculation script for verifying CyberKnife stereotactic radiosurgery (SRS) plans generated using Precision treatment planning system (TPS).

Methodology: The beam data for the reference point were exported as a CSV file and imported into a custom Python script. The Beam parameters such as collimator size, effective depth, off-axis distance, etc. were used to calculate the MU for each beam, which was then compared to the MU calculated by the TPS [2]. To ensure accuracy, beams with a collimator radius smaller than the distance between the beam center and the reference points were excluded in the analysis since it has a large uncertainty and very low dose contribution.

Results: So far, the script has been tested on data from 7 patients. The overall MU difference between TPS and the python script was 0.9%±0.2%(1SD). When excluding beams with collimator radius smaller than the distance between the beam center and the reference points, the ratio of beams with MU difference between 0-3% was increased from 55.3%±14.6%(1SD) to 98.4%±2.7%(1SD). In addition, the MU difference for all beams was within 5%. Figure 1 shows pie charts for the MU difference for one case before and after excluding the beam with collimator radius smaller than the distance to the reference point.

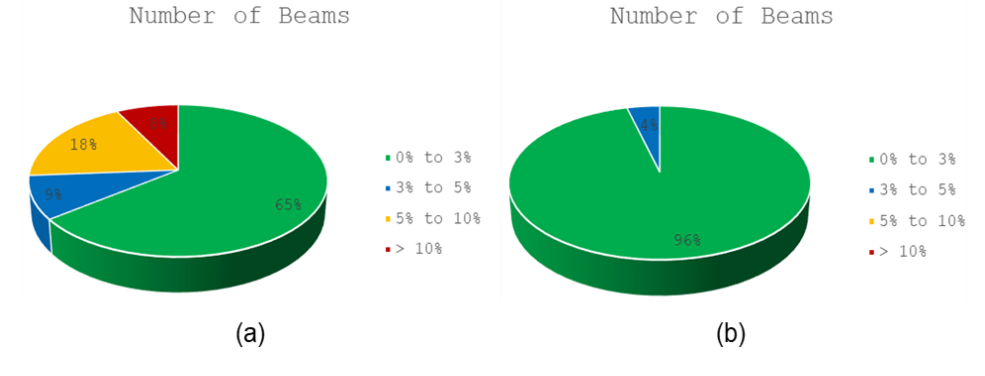


Fig.1: A Pie Char for the MU difference between the python script and TPS for one case when (a) including all beams and (b) excluding beams with a collimator radius smaller than the distance between the beam center to the reference point

Conclusion: The independent MU calculation script provides an additional layer of verification for CyberKnife SRS plans but is not intended to replace patient-specific quality assurance (QA).

- 1. Zhu, Timothy C., et al. "Report of AAPM Task Group 219 on independent calculation-based dose/MU verification for IMRT." Medical physics 48.10 (2021): e808-e829.
- 2. CyberKnfie Physics Essential guide. P/N 1007226A-ENG Accuray (2011).

IMPLEMENTATION OF OPEN-SOURCE QC MANAGEMENT WEB APPLICATION "QATRACK+" FOR ROUTINE QA OF RADIOTHERAPY EQUIPMENT

M. Najem¹

¹ Radiation Oncology Department, King Saud University Medical City, Riyadh, Saudi Arabia

ABSTRACT

Background: Routine quality assurance (QA) for radiotherapy equipment is critical to ensuring the safe and precise treatment of cancer patients [1]. However, recording QA data and analyzing results can be time-consuming, particularly when manual image analysis is performed. QATrack+ (QAT+) is an open-source webbased software designed for QA data management and recording [2].

Objective: This study aims to implement and customize QAT+ in our department to improve the efficiency of routine QA by recording QA data in a central database and automating the analysis for several QA tests.

Methodology: QAT+ was installed on a local server with Ubuntu operating system. Several electronic test lists (QA forms) were developed to record monthly and annual QA checks for Elekta, Varian, and CyberKnife machines. Several Python scripts were implemented in these test lists to automate result calculations and image analysis such as CBCT, kV and EPID image quality and MLC leaf speed tests.

Results: The implementation of QAT+ improved the efficiency and workflow of the routine QA. It reduced the time required to analyze some QA tests, especially those requiring image analysis. For example, the analysis of EPID image quality and scaling tests was reduced from several minutes to only a few seconds. In addition, saving all QA results in one central database made it easier to review historical data to assess any patterns in the QA results and plan for corrective action in advance.

Conclusion: The implementation of QAT+ in radiotherapy centers can enhance efficiency, significantly reduce the time required for routine QA, and facilitate the scheduling of corrective actions through the review of historical QA data.

- 1. Hanley, Joseph, et al. "AAPM Task Group 198 Report: An implementation guide for TG 142 quality assurance of medical accelerators." Medical physics 48.10 (2021): e830-e885.
- 2. Randle, Taylor, "QATrack+" https://qatrackplus.com/ (accessed 14/01/2025).

EVALUATING THE RADIOLOGICAL CHARACTERISTICS AND TISSUE EQUIVALENCE OF POLYLACTIC ACID (PLA)-BASED THREE-DIMENSIONAL PRINTING FILAMENTS FOR RADIOTHERAPY APPLICATIONS

M.S. Bagahezel¹, M.Z. Abdul Aziz¹, G.K. Appalanaido¹, S. Mansor¹

¹ Advanced Medical and Dental Institute (AMDI, IPPT), Universiti Sains Malaysia (USM), Kepala Batas, Pulau Pinang, Malaysia

ABSTRACT

Background: Phantoms in radiotherapy play an essential and crucial role in ensuring dosimetric accuracy and quality assurance by mimicking human tissues. Commercial phantoms often have high costs, low patient customization, and insufficient tissue equivalence.

Objective: This study aims to evaluate the feasibility of using PLA-based filaments to represent soft and bone tissues by studying their radiological characteristics for use as phantoms for radiotherapy applications.

Methodology: Samples of enhanced PLA, PLA doped with aluminium, copper, and bronze (PLA-Pro, PLA/Al, PLA/Cu, PLA/Bronze) with (60%, 70%, 80%, 90%, and 100%) infill densities were 3D-printed by fused deposition modelling (FDM). The samples were CT scanned together with the CIRS CT-ED phantom at (80, 100, 120, and 135) kVp settings. CT numbers (HU) of the samples were determined. The relationships between HU and both density (ρ) and electron density (ED) of CIRS materials were derived to calculate the ρ and ED of the samples. The attenuation coefficients and the product of density and effective atomic number (ρ .Zeff) were also calculated. The relationships between all these radiological properties and infill density were used to calculate the required infill density to mimic certain soft and bone tissues.

Results: The results showed that all the determined radiological characteristics were in the soft tissue range for PLA-Pro and PLA/Al, while they were in the bone tissue range for PLA/Cu and PLA/Bronze. For 120 kVp and 100% infill density, their HU values were 136.11, 170.74, 697.55, and 706.07 HU, respectively. This provides flexibility to mimic a wide range of tissues and masses by adjusting the infill density. With considering all studied properties, adipose, breast, muscle, and liver could be represented by 82%, 86%, 94%, and 95% infill density of PLA-Pro or by 78%, 82%, 90%, and 91% infill density of PLA/Al, respectively. Cortical bone and femoral head could be represented by using 100% infill density of PLA/Cu or PLA/Bronze, while 82% of PLA/Cu and 77% of PLA/Bronze showed the best match to spongy bone.

Conclusion: The study demonstrated the potential of using PLA-based 3D printing filaments to fabricate phantoms with varying soft and bone tissues for radiotherapy applications.

DOSIMETRIC FEASIBILITY OF FAST FORWARD BREAST RADIOTHERAPY USING CO-60 FOR RIGHT-SIDED BREAST CANCER IN A RESOURCE LIMITED SETTING

B.S. Sesath¹, J.H.J.K. De Silva¹, P. Alahakoon¹

¹ Teaching Hospital, Badulla, Sri Lanka

ABSTRACT

Background: The use of Co-60 for hypo fractionated breast cancer radiotherapy offers a promising alternative to conventional fractionation. Hypofractionation reduces treatment duration, enhances patient convenience, and optimizes healthcare resources. While the Fast Forward trial was designed for LINACs, this study evaluates its feasibility for Co-60, which is more accessible in middle-income countries. Given Co-60's unique dosimetric challenges, assessing dose distribution, PTV coverage, and OAR dose constraints is essential for its implementation.

Objective: This study investigates the feasibility of Co-60-based radiotherapy for breast cancer by comparing two regimens: the conventional 40Gy in 15 fractions and the hypo fractionated 26Gy in 5 fractions. A particular focus is placed on analyzing lung and heart dose parameters and ensuring adequate PTV coverage. Furthermore, the analysis explores distribution differences across patient clusters, specifically Wide Local Excision (WLE) and Mastectomy (MA) groups, to identify protocol suitability and enhance treatment personalization.

Methodology: A total of 34 right-sided breast cancer cases were planned by using PCRT-3D for 3D-CRT on a Co-60 machine at Teaching Hospital, Badulla, Sri Lanka. The PTV was contoured according to the Fast Forward protocol. Dosimetric parameters evaluated included homogeneity index (HI), mean heart dose, heart dose, and lung dose metrics.

Results: The HI was higher for MA (mean: 0.59) than WLE (mean: 0.41). Mean heart doses were lower for MA in both 26 Gy (70.19cGy) and 40 Gy (101.71 cGy) compared to WLE. Lung volumes receiving 30% of the dose were similar. WLE had higher heart volumes receiving 5% of the dose for both 26 Gy (5.67%) and 40 Gy (8.67%) than MA (2.57% and 3.71%). No heart volumes received 25% of the dose.

Conclusion: The findings indicate that the Fast Forward trial can be implemented using Co-60 radiotherapy for right-sided breast cancer. However, MA plans demonstrated superior homogeneity and better adherence to heart dose constraints compared to WLE, making them more favorable for hypo fractionated breast radiotherapy. While lung dose differences were minimal, MA plans consistently resulted in lower mean heart doses and reduced heart volume exposure to 5% of the dose. These results suggest that MA plans offer improved cardiac safety in Co-60-based hypo fractionated treatments.

- 1. Planning Pack for the FAST-Forward Trial. Available at: https://dlijoxngr27nfi.cloudfront.net/docs/default-source/defaultdocument-library/fast-forward-planning-pack.pdf. [Last accessed on May 2013].
- 2. Brunt AM, Wheatley D, Yarnold J, Somaiah N, Kelly S, Harnett A, et al.; FAST-Forward Trial Management Group. Acute skin toxicity associated with a 1-week schedule of whole breast radiotherapy compared with a standard 3-week regimen delivered in the UK Fast-Forward trial. Radiother Oncol 2016;120:114-8.

ENHANCING RADIOTHERAPY PRECISION FOR CERVICAL CANCER: MINIMIZING SETUP ERRORS AND REFINING PTV MARGINS

A. Azalmad¹, Y. Elmaadaoui², M. Hilal¹

¹ University Hassan First, Higher Institute of Health Sciences, Settat, Morocco ² Department of Radiotherapy, University Hospital Center Mohammed VI, Marrakech, Morocco

ABSTRACT

Background: Radiotherapy is a fundamental cancer treatment modality that uses high-energy radiation to selectively target malignant cells, often in combination with surgery or chemotherapy. Recent advancements, including Intensity-Modulated Radiation Therapy and Image-Guided Radiation Therapy, have significantly improved treatment accuracy, particularly for pelvic cancers such as cervical cancer. However, setup errors, including patient movement, remain a challenge to the precision of radiotherapy. To address these issues, technologies like portal imaging and the optimization of setup margins are utilized. In Morocco, where cervical cancer is a major health concern, enhancing radiotherapy techniques is crucial for improving patient outcomes. This study aims to improve precision and promote the adoption of advanced treatment methods in Moroccan cancer centers.

Objective: This study aims to improve the precision and effectiveness of radiotherapy for cervical cancer by reducing setup errors, optimizing dose delivery, and minimizing radiation exposure to healthy tissues. It also supports the adoption of advanced radiotherapy techniques in Moroccan cancer centers to enhance treatment quality and patient outcomes.

Methodology: An electronic portal imaging device was used to verify patient positioning in 20 cervical cancer patients, assessing setup accuracy and errors along three axes. PTV margins were calculated using ICRU-62, Stroom's, and Van Herk's formulas. The Van Herk formula, a standard method, accounted for both random and systematic errors to calculate precise margins for accurate dose delivery.

$$PTV margin = 2.5 \Sigma + 0.7 \sigma \tag{1}$$

Results: The findings underscore the necessity of a 6 mm PTV margin in optimizing cervical cancer radiotherapy, ensuring effective tumor coverage while minimizing radiation exposure to healthy tissues. Advanced imaging techniques play a key role in accurately calculating PTV margins, and regular recalculations through daily imaging and weekly assessments are essential for addressing variations in patient positioning.

Table 1 PTV margins calculating for cervical cancer

	Axis	X	Y	Z
Formula				
Van Herk (mm)		6,143	5,7	5,174
Stroom (mm)		5,018	4,68	4,254
ICRU 62 (mm)		2,36	2,2	2,02

Conclusion: This study demonstrates the importance of optimizing PTV margins in cervical cancer radiotherapy. The use of advanced imaging techniques and regular margin recalculations ensures greater treatment accuracy, ultimately improving patient outcomes.

- 1. Azalmad, A., nhila, O., Hilal, M. New Study on Optimizing Cervical Cancer Treatment: Dosimetric Comparison of 3D-CRT, IMRT, and VMAT Techniques at Béni Mellal Oncology Center. *Journal of Obstetrics, Gynecology and Cancer Research*, 2025.
- 2. Alabedi H. Assessing setup errors and shifting margins for planning target volume in head, neck, and breast cancer. J Med Life. 2023 Mar;16(3):394-398. doi: 10.25122/jml-2022-0241. PMID: 37168304; PMCID: PMC10165517.

INVESTIGATION OF DOSE VARIATION IN ADULT NON-CONTRAST HEAD CT FOR RADIATION THERAPY PLANNING: A CASE STUDY FROM SRI LANKA

S. Weerathunga¹, S. Welarathna^{2,3}, B. Perera², P. Malge², T. Bandaranayake², S. Rajamanthri², S. Velautham²

ABSTRACT

Background: Computed tomography (CT) is essential in cancer care, enabling accurate diagnosis, treatment planning, and follow-up. However, excessive radiation exposure to non-target tissues increases the risk of stochastic effects, necessitating dose optimization.

Objective: This study aimed to investigate dose variations in adult non-contrast CT (NCCT) head examinations for diagnostic CT-enabled radiation therapy (RT) planning and to recommend specific optimization approaches to enhance patient protection at a major cancer treatment center in the North Central Province of Sri Lanka.

Methodology: This retrospective analysis included dose reports from 319 adult patients collected between 2020 and 2022. Dosimetric quantities, including the volumetric computed tomography dose index (CTDI_{vol}) and doselength product (DLP), along with acquisition parameters such as kilovoltage peak (kVp), tube current (mA), exposure time, scan length, exposed range, and pitch factor, were extracted. Data analysis was performed using Python, and results were compared with corresponding values reported in the literature.

Results: The analysis revealed consistent acquisition settings (kVp: 120, mA: 300, pitch factor: 0.625, and exposure time: 0.75 seconds per rotation), resulting in a uniform $CTDI_{vol}$ of 66.3 mGy across all examinations. However, DLP values showed substantial variation, ranging from 2175.7 to 4468.0 mGy·cm (mean \pm standard deviation: 3054.8 \pm 340.5 mGy·cm) due to the differences in scan length, which ranged from 35.9 to 69.4 cm.

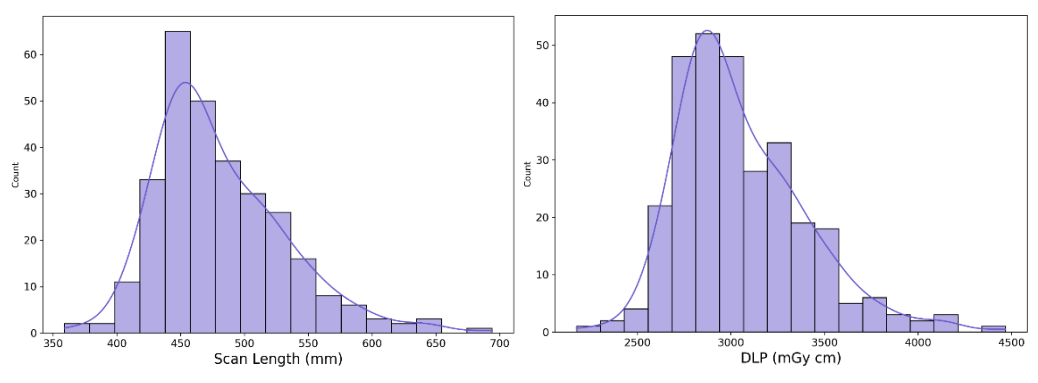


Fig. 1. Frequency distributions of NCCT head RT planning examinations for scan length (left) and DLP (right)

The observed DLP values were substantially higher than those in the literature, indicating the potential need for dose optimization without compromising clinical diagnostic information. Even though the variations in dose may indicate differences in pathology, disease extent, and clinical requirements, the substantial variability in scan length underscores the need for clear justification, as it directly impacts DLP.

Conclusion: These findings highlight the urgent need for personalized CT protocols tailored to patient size and specific clinical requirements to improve patient protection. Therefore, interprofessional collaboration among radiographers, medical physicists, and radiation oncologists is essential for developing optimized RT planning protocols for NCCT head examinations. This study lays the groundwork for comprehensive assessments of patient doses in radiotherapy planning across Sri Lanka, contributing to enhanced patient protection in clinical practice.

Reference: van Elmpt W, Landry G. Quantitative computed tomography in radiation therapy: A mature technology with a bright future. *Phys Imaging Radiat Oncol.* 2018;6:12-13. doi:10.1016/j.phro.2018. 04.004.

¹ Department of Oncology, Teaching Hospital Anuradhapura, Anuradhapura, Sri Lanka

DEVELOPMENT OF A NOVEL 3D-PRINTED HETEROGENEOUS PHANTOM FOR LIVER SBRT DOSE VERIFICATION IN HEPATOCELLULAR CARCINOMA (HCC) TREATMENT

K.V. Anju^{1,2}, M.S. Sreejesh², K. Chiranjib¹, N. Vijayaprabhu³, H.P. Yadav⁴, D. Sharma⁴, V. Subramani⁵, S. Alobaidli²

Amity institute of Applied Sciences, Amity University, Noida, Uttar Pradesh, India
 Kuwait Cancer Control Center, Shuwaikh, Kuwait City, Kuwait
 Jawaharlal Institute of Postgraduate Medical Education & Research, Puducherry, India
 Institute of Liver and Biliary Sciences, Vasant Kunj, Delhi, India
 All India Institute of Medical Sciences, New Delhi, Delhi, India

ABSTRACT

Background: This study focuses on ensuring accurate dose delivery in SBRT for hepatocellular carcinoma (HCC), which is challenging due to complex anatomy.

Objective: The aim of the study is to develop a patient-specific 3D-printed heterogeneous phantom for verifying dose distributions, enhancing treatment precision.

Methodology: The phantom structure was fabricated using a 3D printing technique with Polylactic acid (PLA) filament (Figure A). The tissue compartments were filled with various substances designed to replicate the electron densities of their respective tissues. CT phantom images were analyzed to compare electron density values with literature-reported human tissue data. The dose calculations for SBRT volumetric-modulated arc therapy (VMAT) plans targeting HCC were performed using the Monaco Treatment Planning System (TPS) using Monte Carlo algorithm. Plans were delivered on an Elekta Versa HD Linac (Elekta Medical Systems India Pvt. Ltd., UK). Gafchromic EBT3 film and 0.015 cc ionization chamber measured the dose delivered during treatment. Gamma comparison was performed using the PTW Octavius system (PTW, Freiburg, Germany).

Results: The electron density values for OARs closely matched those reported in the literature. The dose discrepancies measured with the chamber at the isocenter were 0.36%, while at another point within the liver, the discrepancy was 0.67%, and within the heart, it was 1.43% for the VMAT plans. The film analysis showed a gamma pass rate of 99.5% (3%/2 mm) and 97.1% (2%/2 mm) across the plans. The Octavius system achieved a gamma pass rate of 98.3% (3%/2 mm) and 95.4% (2%/2 mm) across plans.

Conclusion: The 3D-printed heterogeneous abdomen phantom is a cost-effective, realistic tool for patient-specific SBRT dose verification in HCC, ensuring precise, safe, and reproducible treatment planning.

References:

1. Ehler ED, Barney BM, Higgins PD, Dusenbery KE. Patient specific 3D printed phantom for IMRT quality assurance. Phys Med Biol. 2014 Oct 7;59(19):5763-73. doi: 10.1088/0031-9155/59/19/5763. Epub 2014 Sep 10. PMID: 25207965.

YOLOv8s-BASED DETECTION OF PROSTATE CANCER USING MULTI-PARAMETRIC MRI

A. Koozari¹, M. Elhaie², I. Abedi²

¹ Department of Medical Physics, School of Medicine, Ahvaz Jundishapur University of Medical Sciences, Ahvaz, Iran ² Department of Medical Physics, School of Medicine, Isfahan University of Medical Sciences, Isfahan, Iran

ABSTRACT

Background: Accurate detection of prostate cancer using multi-parametric magnetic resonance imaging (MRI) is hindered by the subtle contrast between malignant and benign tissues. Deep learning approaches for computer-aided detection (CAD) have gained attention, yet their performance often remains inadequate for routine clinical use.

Objective: The aim of this study was to develop and evaluate a computer-aided detection (CAD) system using the YOLOv8s algorithm for the accurate identification of prostate cancer in multi-parametric MRI scans, with the goal of improving diagnostic precision and supporting clinical decision-making.

Methodology: We implemented a CAD system based on YOLOv8s, a real-time object detection algorithm, to identify prostate cancer in multi-parametric MRI scans. The model was trained on a dataset of 300 MRI scans from patients with biopsy-confirmed diagnoses, where cancer and non-cancer regions were manually segmented by radiologists. Performance was evaluated using mean average precision (mAP), precision, recall, and F1-score metrics.

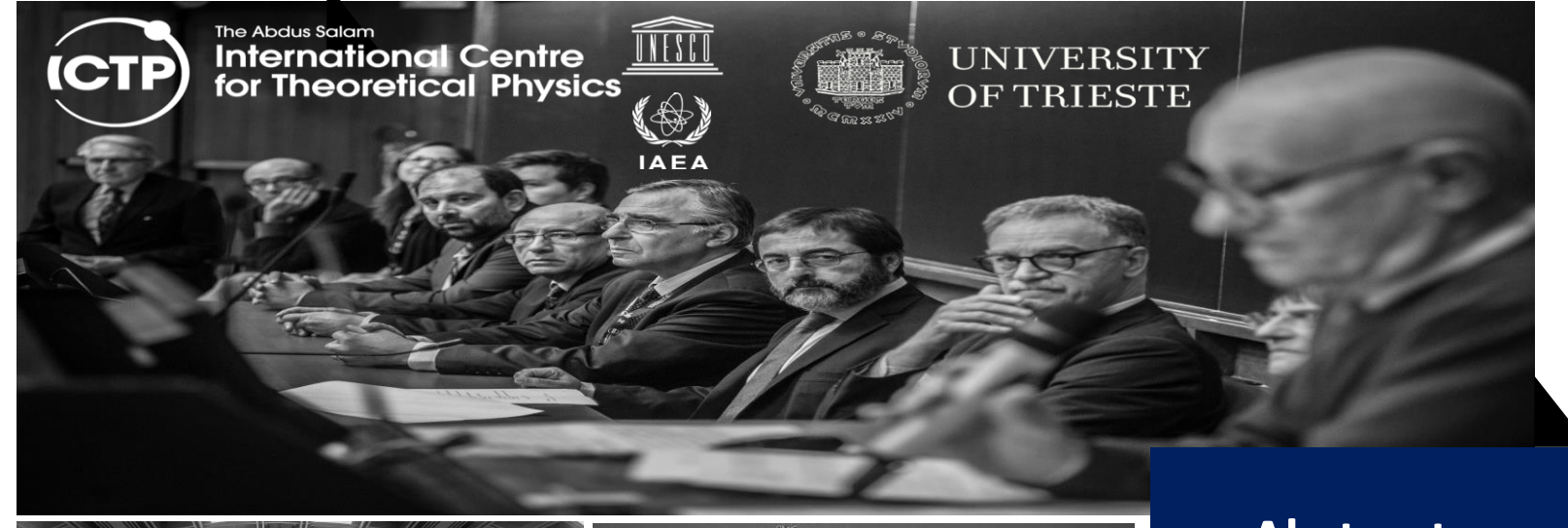
Results: The YOLOv8s model achieved an mAP of 92%, with a precision of 94%, recall of 90%, and F1-score of 92% on a held-out test set. Compared to existing CAD systems, it showed improved localization and classification of prostate lesions, with a notable reduction in false positives.

Conclusion: Our YOLOv8s-based CAD system demonstrates strong potential for prostate cancer detection in multi-parametric MRI, offering high accuracy and real-time processing. Pending validation on larger, diverse datasets, this tool could support radiologists in improving diagnostic precision and streamlining clinical workflows.

References:

1. Lalinia, M., Sahafi, A. Colorectal polyp detection in colonoscopy images using YOLO-V8 network. SIViP 18, 2047–2058 (2024). https://doi.org/10.1007/s11760-023-02835-1.

MEDICAL PHYSICS INTERNATIONAL Proceedings, Vol 1, No. 1; 2025		
	ABSTRACTS OF THE	
ICTP N	MASTER OF MEDICAL PHYSICS PROGRAMM	
	10th Cycle (2022 2024) Twiggte Hely	
	10 th Cycle (2022 – 2024), Trieste, Italy	



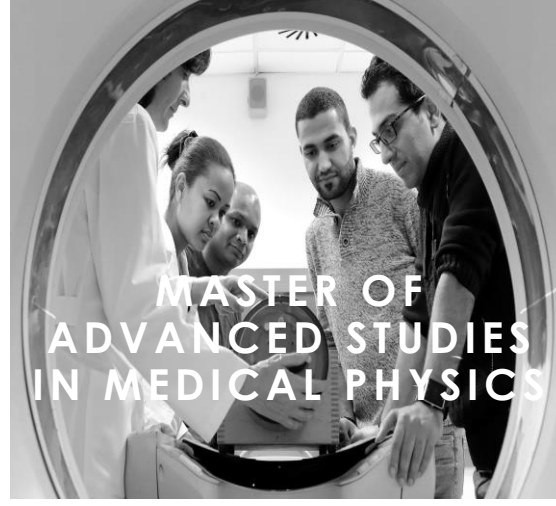




Abstracts Booklet of the MMP Thesis (10th cycles)

The programme is accredited by The International Organization for Medical Physics (IOMP)















Prof. Renata Longo (University of Trieste)

Director of the Master in Medical Physics

Email: renata.longo@ts.infn.it

Office: Via Alfonso Valerio, 2, Edificio F, Department of Physics, University of Trieste, 2nd

Floor



Prof. Renato Padovani (ICTP)

Coordinator of the Master in Medical Physics

Email: padovani@ictp.it

Office:ICTP-Adriatico bulidng-1st Floor



Prof. Luigi Rigon (University of Trieste)

Board Member

Email:luigi.rigon@ts.infn.it



Prof. Fulvia Arfelli (University of Trieste)

Board Member

Email: Fulvia.Arfelli@ts.infn.it



Dr. Paola Bregant-(ICTP)

(University hospital of Trieste)

Board MemeberEmail:paola.bregant@asuits.sanita.fvg.it

Office: Via della Pietà, 4,Ospedale Maggiore, Fisica Sanitaria, 2nd Floor



Prof. Slavik Tabakov (King's College London)

Scientific Adviser

Email:slavik.tabakov@emerald2.co.uk



Prof. Ahmed Meghzifene (IAEA)

Scientific Adviser

Email: a.meghzifene@iaea.org



Dr. Mauro Carrara (IAEA)

Scientific Adviser

Email: M.Carrara@iaea.org



The Master is supported and sponsored by:





International Organization for Medical Physics



European Federation of Organisations for Medical Physics



Institute of Physics and Engineering in Medicine



Italian Association of Medical Physics



Middle East Federation of Organisations of Medical Physics



University Hospital of Trieste

Abstract booklet	
Abstract booklet	#7 (10 th cycles)
Year	2024

Editorial team

Renata Longo,

University of Trieste, Italy

Renato Padovani,

IInternational Centre for Theoretical Physics (ICTP),Trieste, Italy

Hossein Aslian,

Olivia Newton-John Cancer Wellness & Research Centre (ONJ), Melbourne, Australia



Az. Ospedaliero Universitaria Ospedali	Ancona
Riuniti	
Centro di Riferimento Oncologico	Aviano
Az. Ospedaliera Papa Giovanni XXIII	Bergamo
Ospedale S. Orsola	Bologna
Spedali Civili	Brescia
Az. Ospedaliero Universitaria "Arcisp.	Ferrara
Sant'Anna"	
Az. USL Toscana Centro	Firenze
Ospedale Niguarda Ca' Granda	Milano
lst. tumori	Milano
Az.Ospedaliero-Universitaria di Modena	Modena
Az. Ospedaliera S. Gerardo	Monza
Az. Ospedaliero Universitaria Osp.	Novara
Maggiore della Carità	
Istituto Oncologico Veneto	Padova
Ospedale S. Matteo	Pavia
Az. Ospedaliero Universitaria Pisana	Pisa
Az. Ospedaliero Universitario	Reggio Emilia
Ist. Nazionale Tumori Regina Elena	Roma
Az. Ospedaliero Universitaria	Siena
Citta' della Salute	Torino
Ospedale Mauriziano	Torino
Ospedale S. Chiara	Trento
Az. Ospedlaiero Universitaria	Trieste
Az. Ospedaliero Universitaria S. Maria della	Udine
Misericordia	
Az. Ospedaliero Universitaria	Varese
Az. Ospedaliero Universitaria Integrata	Verona
ULSS 6 Vicenza, Ospedale San Bortolo	Vicenza





Tasnim Al Raii tal raii@ictp.it

Supervisors:Dr. Federica Fioroni
Dr. Elisa Grassi

Azienda USL-IRCCS Reggio Emilia, Italy

Red bone marrow dosimetry in Lu-177 Dotatate peptide receptor radionuclide therapy using SPECT-CT imaging

Prospective/Objective: 3D SPECT/CT imaging can assess red marrow absorbed doses, aiding the evaluation of hematological effects in 177177Lu-Dotatate therapy. Comparing different dosimetry methods enhances the understanding of optimal techniques with greater accuracy. Since studies show higher dose values from imaging-based dosimetry compared to blood-based methods, this study employs organ-level dosimetry using VoxelMed2.0 software to process imaging data and acquire cumulated activities in red marrow segmented volumes. Evaluating different methods improves accuracy, while further analysis of individual data points can enhance research and understanding of radiopharmaceutical pharmacokinetics across a range of clinical cases.

Materials and methods: The retrospective images of 28 patients with neuroendocrine tumours that received therapeutic doses of Lu-177-dotatate, acquired from four post therapy 3D SPECT/CT imaging scans at 1h,24h,48h,75h p.i. are computed and analysed. All images were obtained using the same SPECT/CT scanner with the same acquisition and processing parameters that were optimised through a previous work. The segmentation of six volumes of interest drawn manually from L4 to T11 are acquired using Velocity Advanced Imaging workstation 3.2.0. The analysis of fitted time activity curves and cumulated activity in each VOI is done using an in-house built program VoxelMed2.0 developed at Azienda USL-IRCCS, Reggio Emilia, Italy. Finally, these cumulated activities are inserted into OLINDA/EXM version 2.0, for the acquisition of the final absorbed doses.

Results: The overall mean absorbed dose from imaging was 1.11 Gy/7.4 GBq, while blood-based data showed 0.06 Gy/7.4 GBq, agreeing with the assumption made in previous studies that blood-based dose values could be an underestimation for the absorbed doses of red marrow. Although, individual dose values from imaging method seemed to assume an overestimation that requires further investigation. Reanalysis using different computation for the cumulated activity for metastasized patients reduced the overall mean value from imaging to 0.83 Gy/7.4 GBq along with a decreased variability in the data points. Lastly, a comparative analysis of the cumulated activity at two different locations of the aorta are showing a more reliable values for the upper thoracic region with an RSD of 66% as compared to 109% for the lower thoracic region.

Conclusion: The results showed the possibility of finding absorbed doses from imging-based dosimetry with higher values compared with those found using blood-based dosimetry for red marrow under the dosimetrical framework adopted in this study. It proposes alternative computation methods for red marrow cumulated activity based on patients' disease status that could result in a less variable overall mean absorbed dose value for a patient group. Additionally, it suggests the choice of using the upper thoracic aorta region, rather than the lower region, for dosimetric investigations of blood VOIs as a surrogate for red marrow absorbed doses from blood irradiation.



Ilmude C.N. Amadhila iamadhil@ictp.it

Supervisors: Dr. Paola Chiovati Dr. Cristina Cappelletto

Centro di Riferimento Oncologico di Aviano, Italy Comparison between intensity-modulated radiotherapy and volumetric modulated arc therapy using simultaneously integrated boost in head and neck cancer treatment

Prospective/Objective: The increasing patient load in radiotherapy centers requires the selection of techniques that provides optimal dosimetry in terms of target volume coverage, organ at risk sparing and treatment delivery time. Thus this thesis aims to compare the two widely practiced advanced conformal techniques, VMAT and IMRT, in head and neck cancer patients by evaluating the following: how well the dose is conforms to the target, using the conformity number; the uniformity of the dose, using the homogeneity index, the dose received by OARs and the plan complexity of treatment plan by comparing the number of monitoring units and treatment delivery time.

Materials and methods: A retrospective analysis of the treatment plans for five Head and Neck Cancer patients with advanced tumors of the nasopharynx, oropharynx, and hypopharynx. All patients were treated with curative intent using the SIB technique. Treatment was delivered using 6MV IMRT photon beams on a Varian TrueBeam machine. To have unbiased comparison of VMAT and IMRT plan quality, patients initially treated with IMRT technique were also re-planned to use VMAT technique with 6MV. The treatment plans were developed in the Eclipse treatment planning system (TPS) (version 16.1) using the Anisotropic Analytical Algorithm (AAA). Each patients received a prescribed dose to three PTVs; PTV high received 70.95Gy/33 fractions, PTV-intermediate received 62.70Gy/33fractions and PTV-low received 56.10 Gy/33fractions. VMAT plans two full arcs were used whereas IMRT plans used 9 beam fields. The dose constraints aimed for high conformal and homogeneous dose distribution to the PTVs while minimizing dose to the OARs. The dose volume parameters of PTVs, OARs and treatment delivery parameters were compared amongst both the techniques. Statistical analysis was performed using a paired-sample student's t-test.

Results: Both IMRT and VMAT shows no significant differences in terms of conformity, uniformity and the dose received by the OARs. However, there was a significant difference between the two techniques in monitoring units with a p-value of 0.0006 and treatment delivery time with a p value of 0.00002.

Conclusion: In summary, this comparative study between IMRT and VMAT using simultaneously integrated boost for the treatments of head and neck cancer, demonstrated that both techniques provide acceptable target dose coverage and adequate sparing of OARs and normal tissues. However, significant differences were observed in monitoring units (MUs) and treatment delivery time, with VMAT requiring fewer MUs and achieving significantly faster delivery time.



Astanakulov Rukhiddin rastanak@ictp.it

Supervisors:Dr. Marco D'Andrea
Dr. Bartalameo Cassano

Istituto Nazionale Tumori Regina Elena, Italy

Commissioning and clinical dosimetry calibration of a SPECT/CT scanner.

Prospective/Objective: The main objectives of this work were twofold: to perform a comprehensive commissioning of the Siemens Symbia Bold, to confirm compliance with established performance standards and to calibrate the system specifically for clinical dosimetry. This involved determining the scanner's response to radioisotopes and optimizing parameters to ensure reliable dose calculations for patient-specific therapies

Materials and methods: To achieve these objectives, a series of commissioning (intrinsic spatial resolution, extrinsic and intrinsic uniformity, volumetric uniformity) and calibration (system sensitivity factor and dead time) measures were conducted. A Siemens Symbia Intevo Bold SPECT/CT scanner was commissioned according to NEMA protocol and calibration of the aforementioned SPECT/CT and another Siemens Symbia Intevo scanner was carried out, using different phantoms that were employed to evaluate different aspects of the scanner's performance.

System sensitivity: A cylindrical phantom filled with 247 MBq activity of Holmium-166 (Ho-166) was imaged to assess the system's ability to detect and quantify low-level radioactivity. The activity range utilized was 36.67-220.99MBq. The sensitivity calculation was performed by measuring the count rates and comparing them against known activity concentration inside the phantom.

Dead time effects: The CIRS phantom was employed to compute dead time loss. We had three different Ho-166 Microsphere vial sources with activities 10.16, 11.17, 0.11 GBq. The phantom was imaged by inserting the different Ho-166 vial sources consecutively and the corresponding counts per second (cps) were recorded through MIM software.

Results: The commissioning of the Siemens Symbia SPECT/CT scanner involved performing image quality tests and obtaining baseline values for extrinsic, intrinsic, volumetric uniformity and intrinsic spatial resolution. The Siemens Symbia Bold SPECT/CT scanner demonstrated excellent performance in both intrinsic and extrinsic uniformity, with differential uniformity values consistently below 2.5% for CFOV, meeting NEMA standards. Spatial resolution measurements showed mean intrinsic FWHM values below 1.5 mm, while volumetric uniformity achieved a center-to-border ratio close to 1.01, confirming the system's high precision and reliability for clinical imaging applications.

In calibration studies, the sensitivity factor for the Siemens Symbia Bold SPECT/CT ranges from 28.48 to 31.71 cps/MBq, whereas the Siemens Symbia Intevo SPECT/CT demonstrates system sensitivity between 20.02 and 26.48 cps/MBq.

The dead time effects of the Siemens Symbia Bold and Siemens Symbia Intevo SPECT/CT scanners were analyzed. The study demonstrates that dead time losses are negligible, less than 10% at lover activities while revealing a significant increase as activity levels rise, particularly above 0.1 GBq.

Conclusion: The Siemens Symbia Bold SPECT/CT scanner has been rigorously evaluated and successfully commissioned according to NEMA protocols. The baseline results indicated that the Siemens Symbia Intevo Bold SPECT/CT scanner provides consistent and reliable intrinsic and extrinsic performance. The sensitivity calibration demonstrated stable and consistent results across a range of activities. In the dead time effects non-linear models were applied to quantify dead time loss.



Mukhriddin Barotov muxriddin1603@gmail.com

Supervisors: Dr. Veronica Rossetti

A.O.U. Città della Salute e della Scienza di Torino, Turin, Italy

Evaluation and comparison of performances between mammographic machines installed in three different centres, dedicate to clinic and screening

Prospective/Objective: Mammographic systems and digital breast tomosynthesis (DBT) have revolutionized breast imaging, enhancing diagnostic accuracy and early detection of breast cancer. However, variations in equipment performance and optimization across different clinical centers can result in inconsistencies in image quality and radiation dose, ultimately affecting diagnostic reliability and patient safety. This study focuses on evaluating and comparing the performance of mammographic machines across three breast screening and clinical centers, aiming to ensure uniform quality of care and adherence to safety standards.

Materials and methods: The research is divided into two main parts: technical and clinical. The technical part assesses the implementation of the newly DBT protocol developed Italian Association of Medical Physics (AIFM), a quality control (QC) protocol tailored for the DBT modality, and evaluates the performance of the iTAQA software, an innovative tool designed for quality assurance of mammographic systems. The clinical part involves a comprehensive statistical and dosimetric analysis of mammographic examinations conducted in 2023. Parameters such as breast thickness vs radiation dose (average glandular dose) and Diagnostic Reference Level (DRL) were analyzed to identify trends and variations across the three centers.

Results: The results reveal variations in performance and workload among the mammographic systems, showcasing the effectiveness of the AIFM DBT protocol in enhancing image quality and dose precision. The iTAQA software demonstrated its utility as a robust tool for streamlining quality control processes, providing comprehensive insights into system performance. Statistical analysis identified dose distribution patterns, underscoring the critical need for ongoing monitoring and standardization to reduce patient radiation exposure while preserving diagnostic accuracy.

Conclusion: This study concludes with practical recommendations for optimizing mammographic practices and quality assurance protocols. By adopting standardized QC methods and leveraging advanced tools like iTAQA, healthcare providers can achieve consistent performance across mammographic machines, ensuring patient safety and enhancing diagnostic outcomes. These findings contribute to the ongoing efforts to improve breast cancer screening and clinical practices globally.



Marufjon Begijonov begijonovmarufjon@gmail.com

Supervisor: Dr. Lidia Strigari

IRCCS Azienda Ospedaliero-Universitaria di Bologna (University Hospital of Bologna, Italy)

Radiotherapy Treatment Optimization in Patients with Stomach Cancer: A Comparison of Rival Plans

Prospective/Objective: VMAT has the potential to offer advantages, such as reduced treatment delivery time compared with conventional static field intensity-modulated radiotherapy (IMRT). The clinical worldwide use of VMAT is increasing significantly. However, its application to patients with advanced Stomach Cancer is still limited, particularly using auto-planning techniques. This study investigates the performance of several radiotherapy techniques in terms of the capability to fulfill the clinical goals and constraints.

Methodology: This study was conducted in collaboration with IRCCS Sant'Orsola University Hospital and Emam Reza Hospital, which enrolled and treated 30 patients with 3D-CRT diagnosed with advanced stomach cancer. Sixty-five plans (five plans per patient in a subset of 13 patients) were developed and compared in terms of target dose coverage and organ-at-risk (OAR) sparing. Treatment plans were created using the Pinnacle 3 treatment planning system, utilizing auto-planning methods and the Collapsed Cone Convolution algorithm to ensure accurate dose calculation and optimal dose distribution. IMRT plans employed 5-, 7-, and 9-beam configurations, while VMAT plans used single and dual rotational arcs. All plans were normalized to deliver 95% of the prescribed dose to the Planning Target Volume (PTV), adhering to strict dose constraints for OARs. Dose-volume histograms (DVHs) were analyzed to evaluate coverage and sparing, and statistical comparisons among groups in terms of minimum, mean, and maximal dose of PTV and OARs were conducted using the Kruskal-Wallis test.

Results: The selected Stomach cancer patients show a large variability in terms of volume of PTV ranging from 733 to 2124 cm3, partially overlapping OARs like the Heart and Lungs. Three different investigated: schedules were 46Gy/23fractions, 50.4Gy/28fractions, 50Gy/25fractions. According to the analyzed metrics, a decrease in the average maximum dose to the Spinal cord was observed when the number of IMRT beams or the number of arcs increased. A similar behavior was observed in the lungs but not the heart, likely due to the partial overlap with the PTV. However, the KW test did not reveal statistically significant differences among groups, likely due to a limited number of patients. The planned clinical goals were fulfilled with all the techniques in favorable patients (with smaller PTV volume and minimal overlapping with other OARs). In contrast, in complex cases, the overlapping prevented the reach of optimal heart-sparing to the patient and target conformation. The possible solutions to improve planning strategies were analyzed and discussed, considering the entire radiotherapy workflow.

Conclusion: Overall, the intensity-modulated plans are superior to conformal ones. However, the autoplanning technique cannot reach the optimal sparing in stomach cancer patients without using breath-hold and SGRT techniques to reduce OARs and PTV overlapping thus enabling the full benefit of IMRT/VMAT approaches.



Hanna Brynkevich annabrijerry@gmail.com

Supervisor: Dr. Anna Delana

Santa Chiara Hospital, Trento, Italy Evaluation of the dose rate and field size dependence of a liquid filled ionization chamber matrix for pre-treatment verification of stereotactic radiation therapy plan

Prospective/Objective: Pre-treatment verification of the SBRT/SRS treatment plans (TP) require high spatial resolution equipment. Air-filled ionization chambers (IC) have a relatively big volume though can't provide expected spatial resolution. Liquid-filled IC could be an option, but the dose rate (DR) and field size dependencies of the response for such IC have been described in literature. In order for clinical application of the equipment with liquid-field IC DR and field size dependencies should be evaluated, correction factors (CF) calculated, if needed.

Materials and methods: Octavius 1600 SRS matrix (Oct1600) with Octavius II phantom were used to estimate DR and field size dependence of the response of the liquid-filled ICs. A series of measurements of small fields with different DR applied was done. DR were extracted from log files using VB TRFfile software, equivalent square field sizes (Leq) were calculated using MatLAB RTMod software. DR and field size dependencies were evaluated, CFs were calculated. 10 SBRT TPs of pancreas, 15 SBRT TPs of lung, 5 SBRT TPs of brain and 3 SRS TP of brain were irradiated using an Elekta Versa HD linear accelerator. Measurements were done using true composite (TC) and perpendicular field-by-field (PFF) methods of delivery. Dose distributions were measured with Oct1600 and evaluated by VeriSoft using gamma analysis. CFs were applied using Individual and Standardized CF method for single and summarized fields, gamma passing rates (GPRs) were acquired. An additional comparison with retrospective data from Octavius 1500 (Oct1500) pre-treatment verification was done for pancreas and lung cases.

Results: Differences in dose measured by Oct1600 were 0,8-10,4% for 10MV FFF beams and 0,5-5,6% for 6MV FFF beams. For pancreas and brain cases application of CFs increased GPRs for all measured fields. For lung cases application of CFs showed lower GPRs compared to non-corrected fields. Standardized CF method showed higher GPRs as much as single field type of analysis. Comparison with Oct1500 revealed big discrepancies in terms of GPRs due to angular dependence of the Oct1600 response. PFF method showed better results than TC due to angular dependence of the detector's response.

Conclusion: Oct1600 can be used for pancreas and brain SBRT/SRS pre-treatment verification when calibrated with field size and DRs close to the TP's field size and DR or with a proper CFs applied when dose distributions are analyzed. Lung SBRT pre-treatment verification doesn't require any special calibration or CF application.

9 G

Guram Chechelashvili gchechel@ictp.it

Supervisors:Dr. Francesca Palleri

Azienda Ospedaliero Universitaria delle Marche Italy

Establishing reliability in radiotherapy, comprehensive LINAC commissioning and TPS beam model validation

Prospective/Objective: Commissioning a Linear Accelerator (LINAC) is a crucial step in medical physics, requiring a lot of time and effort to ensure safe and accurate treatment delivery. In addition, to gathering a full set of data necessary for patient treatment, it's important to validate these parameters by checking the TPS Beam model with rigorous measurements before treating patients. The objective of this thesis is to highlight the steps needed to achieve the desired outcome: ensuring precision, minimizing errors, reducing risks.

Materials and methods: A new Varian TrueBeam STx LINAC was set up and integrated into clinical use. Acceptance testing was done according to the manufacturer's instructions. Several detectors were used for data acquisition and validation. Absolute dose calibration was done using the MP1 water phantom and a PTW Farmer ionization chamber. Key tools like the BeamScan Phantom, Semiflex ion chamber, Microdiamond and T-ref detectors were used to gather data for commissioning. Dataset included Percentage Depth Dose (PDD) curves, dose profiles, output factors for field size ranging from 2 x 2 to 40 x 40 cm² and the measurements of specific parameters for MLC modelling as Dosimetric Leaf Gap (DLG) and Leaf Transmission Factor (LTF). Measurements were inserted in Eclipse TPS (version 15.6) to configure Analytical Anisotropic Algorithm (AAA) and Acuros XB (AXB) dose calculation algorithms for a 6 MV photon beam. 3D-CRT and VMAT treatment techniques were implemented for clinical use. At first, beam model parameters were checked in Eclipse Beam Configuration module, then the accuracy of calculated dose Profiles and PDD was evaluated using the Profile Comparison Tool. Later the models were validated with dose point measurements in water for open, complex and EDW fields using a Semiflex ion chamber. Additionally, the assessment of the model was performed for VMAT technique according to TG 119 and for clinical plans. Local and Global gamma analysis of VMAT plans with 3%/ 2 mm criteria was conducted with Delta4+. For dose point measurement Cheese and EasyCube phantom were used.

Results: The 6 MV beam was successfully modelled in Eclipse for AAA and AXB algorithms. Dose verification in water and using EasyCube and Cheese phantoms showed mainly less than 2% difference from intended values. Gamma analysis of VMAT plans showed a passing rate higher than 95%, indicating high precision in dose delivery.

Conclusion: Accurate commissioning is a crucial step to ensure the safe use of LINAC systems. By validating the Treatment Planning System and checking the beam models, healthcare professionals can be confident in their ability to deliver the correct dose to the target with precision, reduced uncertainties, and minimized risks of errors in the future. The whole process serves as a comprehensive QA step, during which detailed information is gathered about beam properties, calibration and overall system performance. This study, which focused on 6 MV photon beam, acts as an additional material and offers valuable insights for other physicists involved in future LINAC commissioning and model validation projects.



Sharon L. Gómez-Villegas. sgomez_v@ictp.it

Supervisor: Dr. Roberta Matheoud

Azienda Ospedaliera Maggiore della Carita, Novara, Italy

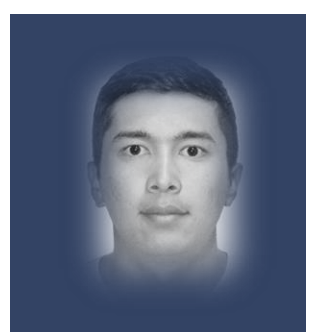
Optimization of counting statistics in nuclear cardiology studies with a solid-state detector gamma camera

Prospective/Objective: CZT-gamma cameras used in Tc99m myocardial perfusion imaging (MPI) enable reductions of administered activity and acquisition times. This study evaluated the feasibility of decreasing the total counts obtained from the left ventricle (LV) while preserving diagnostic accuracy and assessed the impact of this statistical reduction on image quality and clinical parameters. The findings provide insights for optimizing Nuclear Medicine practice.

Materials and methods: A total of 195 patients underwent MPI imaging using the D-SPECT gamma camera with an electrocardiogram-gated protocol. Initially, full count statistics of 1 million counts (Mc) were captured from the LV area. MPI data were processed using a toolkit provided by the manufacturer to reduce the statistical level from 1 Mc to 0.5 Mc. The images were analyzed for Summed Stress Scores (SSS), Summed Difference Scores (SDS), Ischemic Total Perfusion Deficit (ITPD), LV Ejection Fraction LVEF. Concordance between datasets was evaluated using weighted kappa (κw) statistics and Bland-Altman (BA) analysis.

Results: Strong agreement was observed between the 1 Mc and 0.5 Mc datasets for SSS, SDS, ITPD, and LVEF, with concordance correlation coefficients (κ w) of 0.81, 0.64, 0.70, and 0.94, respectively. The bias (B) and limits of agreement for SSS was 0.77 (-2.96; 4.50), for SDS the bias (B) was 0.20 (-4.49; 4.90), for ITPD the bias (B) was 0.38 (-3.82; 4.58), and for LVEF, the bias (B) was -0.001 (-0.07; 0.06), all based on the 0.5 Mc dataset. These results indicate a high level of concordance between the datasets, with minimal bias and narrow limits of agreement.

Conclusion: Myocardial perfusion assessment can be achieved with reduced injected activity and shorter acquisition times, leading to decreased radiation exposure, enhanced patient comfort, and minimized motion artifacts. LV count statistics can be decreased to 0.5 Mc without compromising diagnostic accuracy for key clinical parameters. However, further reductions may be explored.



Kanatbek Karauzokov kkaruzo@ictp.it

Supervisor: Dr. Raffaele Villa

Fondazione IRCCS San Gerardo dei Tintori, Monza, Italy

Image quality in CT: two different approaches for entry-level and advanced evaluation

Prospective/Objective: The study aims to assess CT image quality through two approaches. For entry-level evaluation, the objective is to validate the reliability and accuracy of automated quality control (QC) systems for CT imaging. For advanced evaluation, the study explores variations in image quality across different CT systems, reconstruction algorithms, and vendor technologies from multiple hospitals with the goal of comparing and identifying the optimal protocol parameters for a specific clinical setting.

Materials and methods: Entry-level evaluation was conducted using the Philips CT5300 to perform automated QC assessments, a routine procedure ensuring the consistent performance of CT imaging systems. To validate the system's reliability, manual image quality analysis was performed following the IAEA Human Health Series No. 19 guidelines. For the advanced evaluation, the study targeted Intracranial haemorrhage head protocols, focusing on "encefalo" and "osso" reconstructions. Data were collected from 21 hospitals across Italy, encompassing CT systems from four manufacturers and analyzing 86 CT image datasets. The evaluation compared image quality metrics, including spatial resolution (task transfer function, TTF), noise (noise power spectrum, NPS), and detectability index (D prime), all of which are critical to the diagnostic efficacy of CT imaging.

Results: Entry-level evaluation demonstrated a close alignment between manual measurements and automated QC assessments, validating the reliability and accuracy of the automated QC system for all the evaluated image quality parameters. For advanced evaluation, comparisons of reconstruction algorithms showed consistent CTDI and TTF values while reducing noise, improving the detectability index for the newer generations. Vendor comparisons for the "encefalo" protocol highlighted the overall performance of Vendors 2 and 3. In the "osso" protocol, Vendor 2 showed higher detectability and overall balance, while Vendor 1 demonstrated improved noise reduction and Vendor 4 offered higher resolution. Protocol optimization revealed that some hospitals achieved a balance between minimizing radiation dose and maintaining high image quality, while others showed moderate performance.

Conclusion: This study validates the reliability of our automatic QC system for entry-level CT image quality evaluation, showing strong alignment with manual quality control methods based on international guidelines. For advanced evaluation, the results highlight how modern reconstruction algorithms and vendor technologies improve diagnostic image quality without increasing radiation dose, achieving a critical balance between resolution, noise reduction, and detectability. Vendor comparisons reveal unique strengths in dose optimization, noise management, and image quality. By leveraging these strengths, healthcare providers can improve image accuracy while maintaining radiation dose. Optimization analysis emphasized the importance of dose and slice thickness in achieving optimal results.



Jerome Kenfac Makeng kenfacj@gmail.com

Supervisor: Dr. Gianfranco Loi

Azienda Ospedaliero Universitaria Maggiore della Carità di Novara

Clinical commissioning of four Varian TrueBeam Linacs: an experience from a single multi-site institution

Prospective/Objective: This study presents the clinical commissioning process of four Varian TrueBeam LINAC across a multi-site healthcare institution. The goal was to ensure consistency, accuracy and interoperability to achieve high-quality radiotherapy services across all locations. Key aspects of commissioning included beam data collection, dose calibration, TPS beam modelling and its validation for VMAT delivery. Challenges specific to the multi-site deployment, including standardization of workflows, cross-site data harmonization, and staff training, were addressed. The experience highlights the importance of a collaborative, structured approach to ensure uniformity and accuracy in radiation treatment delivery across different sites.

Material and methods: In this work, 6MV WFF and FFF photon beams were commissioned. All the linacs were equipped with the 120 Varian Millenium MLC, and some features (RapidArc, kVCBCT and EPID). The commissioning process took on average five weeks per unit, it started on January and finished in November of this year. Machine's mechanical/geometric performances and VMAT capabilities were preliminary checked during the acceptance tests. Beam data collection, including output factors was performed using the two different water phantoms available on site. PDDs, crossline/inline, diagonal profiles for field sizes ranging from 1x1 cm2 to 40x40 cm2 were acquired with different setups analysed and imported in the Raystation TPS to generate the beam models. Different specific detectors were available for relative dosimetry of small field sizes. Relative dosimetry of large field sizes was performed by the IBA CC13 chamber, used also for absolute dose calibrations. The same instrumentation was used for TPS beam models basic validations. The Sun Nuclear ArcCheck 3D diode array was employed for VMAT commissioning and validation by end to end testing (E2E) geometric and real clinical scenarios. A beam meta-model pooled on all the collected data has been commissioned and validated against customized beam models achieved from the single beam specific data to assess the agreement and interoperability throughout all the installed TrueBeams.

Results: The beam quality index (%dd(10)) and PDD measurements for TrueBeams units showed excellent agreement with Varian Golden Beam Data, with deviations of less than 0.5%. Crossline and inline profiles were measured for large and small fields, correcting for detector volume effects. Output factors across sites were consistent, with a 2% lower OF for TB1 due to uncertainties in the Razor diode measurement. All measurements were within 1% of published data. Customized models developed for TB1, TB2, and TB3, and the meta-machine model showed a level of agreement better than 0.5%. Calculated output factor in the worst case scenario (1x1 cm2) resulted within 2% respect the measured ones for all the machine sample. The meta-machine model demonstrated strong agreement with the customized models in basic in water validations and in E2E VMAT plans. Even in the most complex scenarios the passing rates of global gamma (2%,2mm) resulted above 95%. Similar high passing rate were found comparing the dose distribution calculated interchanging the models on real clinical cases with tighter (1%, 1 mm) criteria, showing the complete interoperability of the machine models.

Conclusion: The TrueBeam systems demonstrated consistent beam qualities and output factors across multiple sites, in good agreement with Varian Golden Data and external audits, confirming reliable and robust VMAT performances in clinical environments. A single beam meta-model generated pooling the data from all the machine was validated successfully for all the commissioned units.



Javin H. Luke
javin.luke@gmail.com

Supervisor: Dr. Sabina Strocchi

Ospedale di Circolo e Fondazione Macchi, Varese, Italy

Development of an updated quality control protocol (QCP) for fixed-type digital X-ray equipment managed by Ospedale di Circolo e Fondazione Macchi, Varese, Italy

Prospective/Objective: Digital X-ray machines are rapidly evolving, necessitating that our QCP be adapted to ensure optimal performance and radiation safety for all stakeholders. The current QCP is becoming outdated since newer equipment is added to the hospital network on a yearly basis. This situation underscored the need to update the current protocol to reflect the latest technological advancements and best practices. The objective of this study was to develop an updated QCP for the fixed-type digital X-ray equipment under the hospital's management.

Materials and methods: This qualitative study was divided into two parts. In the theoretical half, the theoretical and regulatory frameworks were established, and the main elements of the QC process were identified. These defined what QC meant in the context of this research. A literature review was done to determine current best practices and standards. In addition, tests were jointly selected from the literature with the relevant Medical Physics Expert (MPE).

In the practical section, three surveys were carried out in the hospital network to establish baseline conditions in terms of resources and constraints. The current protocol was reviewed for the same reason. Using this data, a gap analysis was done to identify discrepancies between the current protocol (current state) and the current best practices (desired state). Acting on the results, a draft protocol was designed, and the new tests were conducted to verify their practicality and to uncover any unforeseen factors.

Results: Findings revealed the importance of accounting for the bucky attenuation during the determination of the Exposure Index (EI) accuracy on radiographic equipment. Second, more research is needed to establish limits and typical values for neurological studies performed on angiographic equipment for the *Air Kerma Rate (AKR) at the patient entrance* and the *AKR at the image receptor entrance* tests. And third, the success of interoperability tests during acceptance depends on both technical and non-technical factors such as organization and management.

Conclusion: An updated QCP for fixed-type digital x-ray equipment was developed through this research. The protocol covered acceptance and routine testing for radiographic and radioscopic equipment, excluding computed radiography systems due to their obsolescence. Notable innovations include the introduction of interoperability testing and a flexible test-level framework for enhanced adaptability. The practical testing was considered an indispensable part of the update process, emphasizing the need for greater time allocation to it. To strengthen the update process, the addition of a comparative analysis and staff feedback mechanism were recommended. The use of the updated protocol is expected to improve patient safety and diagnostic accuracy. Future research is recommended to assess its performance after implementation, reinforcing the concept of QC in medical x-ray imaging as a continuous cycle of improvement.



Aaron Fulgence Mayima Mboungou amayima@ictp.it

Supervisor:Dr. Maria Rosa
FORNASIER

The University Hospital of Trieste

Optimization of a quantitative SPECT/CT reconstruction protocol: phantom measurements and preliminary clinical evaluation.

Prospective/Objective: Quantitative SPECT/CT measures medical images to accurately evaluate biological processes and pathological conditions and is useful both in diagnosis and in therapy. Nowadays, gamma camera manufacturers have produced iterative quantitative reconstruction algorithms, that model physical characteristics of the acquisition process and incorporate the correction needed for quantitative SPECT, such as collimator-detector response, photon scatter, photon attenuation, partial volume artefacts. Our objective was to evaluate the accuracy of an available quantitative software (xSPECT), optimize its configuration and extend the results to clinical activity focusing on quantitative SPECT/CT examinations for the diagnosis of cardiac amyloidosis.

Materials and methods: After calibrating the system, we prepared a NEMA IEC phantom, filling the spheres and the background compartment with homogeneous solutions of 99mTc-pertechnetate having a concentration of 35.1 kBq/ml and 5.8 kBq/ml, respectively, so that the sphere-to-background ratio was approximatively 6:1. We acquired the phantom and reconstructed the images by xSpect. The optimization of reconstruction parameters, such as number of iterations, subsets and extent of the applied smoothing filter was based on measuring their impact on quantitative metrics, that is Standardized Uptake Value, recovery coefficients, relative deviation, hot spot contrast, spatial resolution and coefficient of variation. In the final part, we performed some preliminary evaluation on the reconstructed clinical images.

Results: For hot spheres, we found that maximum activity concentration provides more accurate estimation of the real activity concentration than peak or average values, that underestimate it. The deviation from the real value increases while the diameter of the spheres decreases, as effect of the spill-out. Moreover, we found that the maximum activity concentration for the spheres of smaller diameters is closer to the real value in less smoothed reconstructions (10 mm filter); for the spheres of largest diameters, the evaluated concentration is closer to the real value when applying 13 mm filter; the application of 16 mm smoothing gives the worst results. We found that iterations increase does not improve accuracy but introduce noise. Recovery coefficients and hotspot contrast reveal size-dependent effects of partial-volume correction. Background activity was best evaluated by the average concentration, unaffected by reconstruction parameters. The overall findings suggest that the best reconstruction has 24 iterations, 1 subset and 13 mm Gaussian filter. However, in the preliminary evaluation of few clinical cases, the optimal setting seems to be 20 iterations, 1 subset, 10 mm filter, that balance noise and details smoothing; increasing the iterations leads to very noisy images and increasing the Gaussian filter smooths to much the volumes with high uptake.

Conclusion: This study allowed us to evaluate the performance of the quantitative algorithm xSpect and to establish the best reconstruction parameter for a phantom study. Application to clinical images leads to different results and highlights the need for further analysis with both antropomorphic phantoms and patients images. Moreover, several adjustments to acquisition protocols in terms of acquisition time and pixel sizes are essential for accurate quantitative assessments in clinical practice.



Mohammad
Mehrpouyan
mehrpouyan.mohammad@
gmail.com

Supervisor: Dr. Lidia Strigari

IRCCS Azienda Ospedaliero-Universitaria di Bologna (University Hospital of Bologna, Italy)

Stereotactic Body Radiotherapy Treatment for Bone Metastasis: An End-to-End Study

Prospective/Objective: Stereotactic body radiotherapy (SBRT) has emerged as a preferred modality for managing bone metastases, offering improved local tumor control and reduced toxicity to surrounding healthy tissues. However, accurate dose delivery remains critical due to the proximity of organs at risk (OARs), such as the spinal cord. This study aimed to validate the accuracy and reproducibility of SBRT for bone metastases using an end-to-end analysis with a custom 3D-printed phantom. Specific objectives included optimizing tumor coverage while sparing OARs under varying prescription doses and verifying treatment delivery accuracy across different beam modalities.

Materials and methods: A 3D-printed bone phantom, designed to mimic the anatomical structure and radiological properties of bone and target, underwent the complete radiotherapy workflow for SBRT. Single-fraction treatments were planned at prescription doses of 18 Gy, 22 Gy, and 27 Gy, using both Flattening Filter Free (FFF) and standard Flattened Filter (FF) photon beams. Treatment planning based on a single arc and Volumetric Multiple Arc Therapy (VMAT) technique, was conducted using the Pinnacle Treatment Planning System, employing the Collapse Cone Convolution algorithm and autoplanning engine. Plans were scored based on clinical objectives and delivered for experimental validation.

Dose measurements were performed using Gafchromic films placed in transverse and sagittal planes, focusing on the small lesion site. The films were calibrated for photon energies up to 30 Gy and scanned with an Epson 1680 Pro scanner. Gamma Index analysis and dose profile comparisons were conducted using PTW MEPHYSTO software and VeriSoft Patient Plan verification tools, which assessed 2D/4D pretreatment IMRT and VMAT plans. Multiple setup configurations were tested to evaluate the impact of phantom positioning on dose delivery accuracy.

Results: Higher prescription doses delivered with FFF beams demonstrated faster treatment times and steeper dose gradients, particularly at the axial center of the irradiation field. Gamma Index analysis for comparing sagittal and transverse dose distributions (>90% for all the deliveries and beams) indicated strong agreement between planned and delivered doses, with deviations well within acceptable thresholds. Variations in phantom positioning occasionally resulted in suboptimal OAR sparing; however, repeated irradiations minimized discrepancies and highlighted key factors for improving setup reproducibility. The custom-designed phantom proved effective for simulating realistic clinical scenarios and identifying potential pitfalls in treatment planning, setup imaging and delivery.

Conclusion: This study provides a comprehensive technical validation of SBRT for bone metastases using a novel 3D-printed bone phantom. Unlike traditional phantom studies, the anatomically accurate design enhanced simulation fidelity, aiding in precise dose calculation and delivery. The use of Gamma Index analysis for comparing sagittal and transverse dose distributions underscores its utility in three-dimensional treatment validation. The findings demonstrate the effectiveness of FFF beams for high-dose SBRT while emphasizing the importance of meticulous setup and verification processes in the entire radiotherapy workflow. This study supports the ongoing refinement of SBRT protocols to achieve superior clinical outcomes in bone metastasis treatment.



Linda Mission

Imission@ictp.it

Supervisors: Dr. Luca Nocetti

Azienda Ospedaliero-Universitaria di Modena, Italy

In vivo evaluation of noise magnitude in Liver CT imaging and how it is influenced by patient diameter across different CT scanners and protocols.

Prospective/Objective: Implementation of dose optimization based on ALARA principle is necessary for patient safety in CT imaging. However, low radiation doses result in increased image noise which reduces visibility and contrast of soft tissues in CT images. Patient size is an important aspect in CT imaging as it affects both radiation dose and image quality. Large patients attenuate more x-rays reducing the photons that reach the detector resulting in increased image noise. The AEC and IR algorithms are used in CT to reduce radiation doses and image noise for different patient sizes so that images of acceptable diagnostic quality are acquired at low doses. However, the IR does not completely eliminate image noise, rather the noise is just reduced to a certain extent. The objective of this study is to evaluate the noise magnitude in abdomen CT imaging and how patient size influences the image noise in different CT scanners and protocols.

Materials and methods: Abdomen CT images of 213 patients acquired from GE LightSpeed VCT, GE Optima CT660, and Siemens SOMATOM Definition Edge CT scanners retrieved from PACS were used in the study. The patient size was estimated in terms of water equivalent diameter (D_w) and effective diameter. CTDI_{vol} and SSDE were the dose metrics used to calculate CT radiation doses. The CTDIvol values were extracted from image DICOM header and RDSR. SSDE values were calculated as the product of CTDI_{vol} and conversion factors. Parameters required for the estimation of noise magnitude (standard deviation of mean CT number), SNR, D_w, mis-centering and effective diameter were extracted from the patient images using semi-automatic ImageJ macro. Three circular ROIs were placed in homogenous regions of the liver to measure noise and SNR. The variation of noise, SNR, CTDI_{vol} and SSDE values was compared for various patient sizes across CT scanners and protocols. The variation of SNR versus dose metric parameters across CT scanners and protocols was also assessed.

Results: A positive linear correlation was found between noise magnitude and D_w (p<0.001). SNR decreases with increasing D_w while $CTDI_{vol}$ and SSDE increased with D_w in all scanners. Correlation coefficients for relationship between SNR and D_w were -0.86 (p<0.001), -0.64 (p<0.001), -0.68 (p<0.001) for SOMATOM Definition Edge, LightSpeed VCT and Optima CT660, respectively. The first scanner showed high SNR values compared to the remaining two at diameters below 34 cm although with a highest trendline slope value of -0.3519 compared to others. Above 34 cm all scanners had similar SNR values although most of scans for SOMATOM Definition Edge were obtained at lower doses.

Conclusion: Significant relationship between noise and patient diameter was found as well as between dose parameters and patient diameter. According to the protocols in use, SOMATOM Definition Edge performed better than the LightSpeed and Optima scanners in terms of SNR and patient doses.

This study show that simple tools and techniques which can be easily reproduced can be used to assess different parameters of medical imaging systems which can help in dose optimization leading to high diagnostic accuracy

Calibration of linear accelerator with various ionization chambers

Prospective/Objective: The objective of this study is to evaluate the calibration of a linear accelerator using different ionization chambers. The focus is on comparing dose measurements obtained with RW3 slab phantoms and water phantoms. The study aims to assess the consistency and accuracy of dose measurements across different phantom materials and investigate the response of six ionization chambers under these conditions, following the TRS-398 protocol for calibration.

Eliza Nurlan kyzy elijenishbekova@gmail.com

Supervisor: Dr.Francesco Ziglio

Ospedale Santa Chiara, Trento, Italy Materials and Methods: Calibration measurements were performed on a Versa HD Linear Accelerator, including percentage depth dose (PDD), beam quality index TPR_{20,10}, and all relevant correction factors for four beam energies: 6 MV, 10 MV, 6 MV FFF, and 10 MV FFF. The ionization chambers used were the PTW Farmer 30013, Semiflex 31013, PinPoint 3D 31016, Semiflex 31010 (SN004482 and SN004481), and Semiflex 3D 31021. The PTW UNIDOS E electrometer was used to accurately measure the charge collected by the ionization chambers during the calibration process. Two types of water phantom (PTW MP3-M and MOD32 WP) and an RW3 slab phantom were employed for the measurements.

Results: The PDD measurements for 6 MV and 10 MV showed less than 1% difference between the two phantoms (RW3 and water phantom). For the beam quality index TPR_{20,10}, all six ionization chambers produced nearly identical values, demonstrating excellent reproducibility. This consistency indicates that the beam quality index is stable and reliable when measured in RW3 and water phantoms. The correction factor for the slab phantom to water phantom was measured with the Farmer 30013 under identical temperature and pressure conditions on the same day. Absorbed dose measurements to water showed high consistency across all ionization chambers and beam energies, with small variations attributed to chamber-specific characteristics, such as the sensitive volume size. As a result, the output factor was as expected, with both Semiflex 31010 (SN004481 and SN004482) chambers demonstrating ideal results, confirming their high accuracy, the ion chambers Farmer 30013 and Semiflex 31013, respectively, also had a good result, ion chambers Semiflex 3D 31021 and PinPoint 3D 31016, designed for small-field dosimetry got slightly lower output.

Conclusion: This study provides a detailed evaluation of LINAC Versa HD calibration using different phantoms and ionization chambers. The findings highlight the reproducibility and accuracy of dose measurements across various chamber types and phantom materials, enhancing our understanding of dosimetric precision in clinical settings. The study underscores the importance of chamber specifications and applications in ensuring accurate and reliable calibration of linear accelerators.

Development and Validation of a Software Comparison Framework: An Empirical Analysis of the Monaco and Raystation TPS

Prospective/Objective: To meet the evolving clinical needs of the radiation oncology unit at the at the SCB, they are phasing out of a soon to be non-manufacturer supported TPS. Considerations are underway for increasing the license count between two other TPS to fill the need. These TPS were Monaco by Elekta® for which there are currently a small number of licenses for use and RayStation 2023B by RaySearch Laboratories® which is currently primarily used by the radiation oncologist for contouring. The objective of this study was to create a novel method to compare the performance of the two TPS being considered for increased license purchase and generate a feasible choice besed on the information gathered.

Materials and methods: The patient data to be used was first gathered; the RT department database was filtered to show the most frequently treated anatomical groups using a conventional Linac and which were planned on Monaco; they were the prostate, beasts, pelvis excluding prostate, lungs lungs including Lymphomas where the treatment boundaries extend into the lungs and liver sites. A sample group of 12 plans per site were chosen for this study. Pretreatment QA was done under the guidelines of the AAMP TG -218 [1]; using the Elekta VersaHD™ Linac and the ArcCHECK diode detector array Phantom and its corresponding software and guidebooks [2] [3]. With this information used as a base model, the standardized framework was created to assess all plans using a decision tree structure to handle the data permutations to streamline full results generation. All plans chosen were jointly approved by the patient's attending radiation oncologist and assigned medical physicist. The treatments were already carried out prior to this study. For the sake of uniformity all treatment parameters for each plan remained the same, including the inverse planning method. The optimization methods were different, however, but this was based on the program's user interface setup. Gamma analysis information was collected and compared using both the normative comparison methods [1][2] and newly devised boundaries to give quantitative results. Qualitatively, the plans were compared using the plan's achieved dose data; DVH, dose distribution and mandated dose criteria, but with further newly devised analytical methods based on OAR radiobiological data to standardize the scrutiny. A final method was also created to combine these outcomes to give holistic results.

Results and Conclusion: A decision tree was created from the amalgamated methods and processed to show and explain the comparison framework. The outcome of using it for this study provided robust information on both TPS, allowing for an easy practical analysis for both on conventional Linacs, in a clinically relevant capacity. Insight into the performance of both TPS showed the dynamic-MLC treatment mode used for the breasts while alluding to RayStation qualitatively, lacked adequate statistical data and needed further studies to better define an answer. RayStation however, had a better overall performance for this study when VMAT was considered over all regions for FFF and non-FFF beams.

Adam Superville supervilleadam@gmail.com

Supervisor: Dr. Cristian Toraci

Spedali Civili, Brescia, Italy



Lesly Tsoptio
tsoptiolesly97@gmail.com

Supervisor: Dr. Angelo Monti

ASST Grande Metropolitano Niguarda, Milan, Italy

Commissioning of a new Linac Versa HD for VMAT Treatments

Prospective/Objective: Advanced radiotherapy techniques like Volumetric Modulated Arc Therapy (VMAT) improve treatment outcomes and minimize side effects to OARs. However, VMAT requires a dedicated Linac capable of precise MLC control and accurate beam modulation. This work focuses on the commissioning of a new Versa HD Linac for VMAT treatments.

Materials and Methods: Elekta-Linac beam data were acquired, including scanned data (PDDs, profiles, and diagonals) and non-scanned data (scatter factors, absolute dose). These data were integrated into the Monaco TPS to create a beam model, to be validated by comparing planned and measured dose distributions. Absolute dose accuracy was evaluated using the percentage of relative error, while PDDs and profiles were analyzed with a 2D gamma index (BDAS software; acceptance criteria: 2%/2mm and 1%/1mm). MLC modeling was verified focusing on a "Four L test", which uses four segments with L-shaped fields and dose profiles were compared using ScandiDose software. AAPM TG-119-recommended tests were performed using a Delta 4 phantom for 3D measurements, with measured and calculated profiles analyzed with ScandiDose's 3D gamma index (global, 3%/3mm and 2%/2mm; 10% cut off) and a PTW Matrix phantom for single point measurements.

Results: Monaco-calculated and measured absolute doses demonstrated excellent agreement, with differences within $\leq 0.64\%$. Relative dose accuracy was consistently high across all field sizes, with PDD passing rates ranging from 95% to 97% and profile passing rates reaching 100%, particularly for 3×3 cm² and 10×10 cm² fields. MLC modeling assessed through the Four L test showed discrepancies of less than 0.2% in the 6 MV FFF Picket Fence and Leaf Groove regions. 3D measurements from AAPM TG-119 tests achieved gamma passing rates above 99.5%, with low confidence limits of 0.46% for 6 MV and 0.53% for 6 MV FFF under the 3%/3mm criterion while point measurements exhibited minimal confidence limits of 0.03 for both energies. These results highlight the TPS's outstanding consistency and reliability in accurately modeling both simple and complex treatment plans for 6 MV and 6 MV FFF beams.

Conclusion: The results demonstrated the clinical reliability and accuracy of the Versa HD Linac and Monaco TPS for VMAT treatments, supporting their clinical implementation.



ICTP- Strada Costiera, 11 I-34151 Trieste Italy mmp@ictp.it



Via Alfonso Valerio, 2, Department of Physics, University of Trieste, 34127 Trieste, Italy



Master in Medical Physics Alumni Association (MMPAA)



ICTP & UniTS's Medical Physics Graduates (IUMPG)

INFORMATION FOR AUTHORS

MEDICAL PHYSICS International Proceedings

PUBLICATION OF CONFERENCE PROCEEDINGS AND DISSERTATION ABSTRACTS

A special feature of Medical Physics International (MPI) Proceedings (online at www.mpijournal.org) is the publication of abstracts from IOMP's International Conference on Medical Physics (ICMP) and IUPESM World Congresses (WC), Conferences of IOMP regional and national organizations, and dissertation abstracts for recent graduates in medical physics or closely related fields. This is an opportunity for recent graduates to inform the global medical physics community about their research and special interests.

Abstracts for ICMP and WC conferences should be submitted by conference organizers. In the case of

dissertation abstracts/proceedings, authors must submit their abstract along with a letter/message requesting and giving permission for publication, stating the field of study, the degree that was received, and the date of graduation. The abstracts must be in English and no longer than 2 pages (using the MPI Proceedings template) and can include color images and illustrations. The abstract document should contain the thesis title, author's name, and the institution granting the degree.

Complete information on manuscript preparation is available in the INSTRUCTIONS FOR AUTHORS section of the online journal: www.mpijournal.org.

INSTRUCTIONS FOR AUTHORS

The goal of the Medical Physics International Proceedings (http://mpijournal.org) is to publish abstracts and/or proceedings of IOMP's International Conference on Medical Physics (ICMP) and IUPESM World Congresses (WC), Conferences of IOMP regional and national organizations, and dissertation abstracts for recent graduates in medical physics. This will enhance medical physics education and professional development on a global basis. There is a special emphasis on general review articles, reports on specific educational methods, programs, and resources.

In general, this publication will be limited to resources that are available at no cost to medical physicists and related professionals in all countries of the world. Information on commercial educational products and services can be published as paid advertisements.

A special feature of the IOMP MPI Proceedings will be the publication of thesis and dissertation abstracts for recent doctoral graduates, specifically those receiving their doctoral degrees in medical physics (or closely related fields) in 2010 or later.

MANUSCRIPT STYLE

Manuscripts shall be in English and submitted in WORD. Either American or British spelling can be used but it must be the same throughout the manuscript. Authors for whom English is not their first language are encouraged to have their manuscripts edited and checked for appropriate grammar and spelling. Manuscripts can be up to 10 journal pages (approximately 8000 words reduced by the space occupied by tables and illustrations) and should include an unstructured abstract of no more than 100 words.

The style should follow the template that can be downloaded from the website at:

http://mpijournal.org/authors submitapaper.aspx

ILLUSTRATIONS SPECIAL REQUIREMENTS

Illustrations can be inserted into the manuscript for the review process but must be submitted as individual files when a manuscript is accepted for publication.

The use of high-quality color visuals is encouraged. Any published visuals will be available to readers to use in their educational activities without additional approvals.

GUIDELINES ON CONFERENCE ABSTRACTS:

- 1. MPI publishes only abstracts of conferences (Book of Abstracts)
- 2. Word limit for abstracts 350 words (1 page per abstract)
- 3. Template for the abstract is prepared by the conference organizers and does not need to follow specifically the MPI manuscript template.
- 4. Book of Abstracts is prepared entirely by the conference organizers.
- Conference organizers should send to MPI a large PDF file with all abstracts and the file is added as an Annex to MPI

REFERENCE WEBSITES

Websites that relate to the abstract's topic and are sources for additional supporting information should be included and linked from within the article or as references.

EDITORIAL POLICIES, PERMISSIONS AND APPROVALS

AUTHORSHIP

Only persons who have made substantial contributions to the manuscript or the work described in the manuscript shall be listed as authors. All persons who have contributed to the preparation of the manuscript or the work through technical assistance, writing assistance, financial support shall be listed in an acknowledgements section.

CONFLICT OF INTEREST

When they submit an abstract, whether an article or a letter, authors are responsible for recognizing and disclosing financial and other conflicts of interest that might bias their work. They should acknowledge in the manuscript all financial support for the work and other financial or personal connections to the work.

All submitted abstracts must be supported by a document (form provided by MPI) that:

- Is signed by all co-authors verifying that they have participated in the project and approve the manuscript as submitted.
- Stating where the manuscript, or a substantially similar manuscript has been presented, published, or is being submitted for publication. Note: presentation of a

paper at a conference or meeting does not prevent it from being published in MPI and where it was presented can be indicated in the published manuscript.

- Permission to publish any copyrighted material, or material created by other than the co-authors, has been obtained.
- Permission is granted to MPI to copyright, or use with permission copyrighted materials, the manuscripts to be published.
- Permission is granted for the free use of any published materials for non-commercial educational purposes.

COMPARATIVE ASSESSMENT OF AVERAGE GLANDULAR DOSE IN DIGITAL BREAST TOMOSYNTHESIS AND FULL-FIELD DIGITAL MAMMOGRAPHY IN OMAN

N. Al Maymani¹, R. Al Mamari², A. Al Jabri³, S. Kheruka¹, N. Al Makhmari¹, H. Al Saidi¹, S. Al Rashdi¹, A. Al Balushi¹

Radiology and Nuclear Medicine Department, Sultan Qaboos Comprehensive Cancer Care and Research Centre (SQCCCRC), University
Medical City, Muscat, Oman.

³ Physics Department, College of Science, Sultan Qaboos University, Muscat, Oman.

³ Radiology and Molecular Imaging Department, College of Medicine, Sultan Qaboos University, Muscat, Oman.

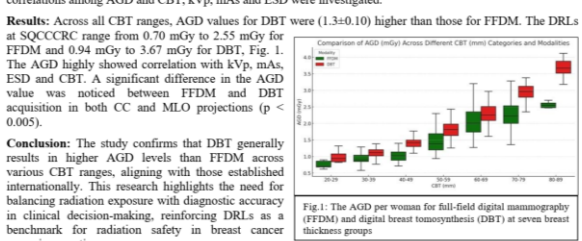
ABSTRACT

Background: With the integration of Digital Breast Tomosynthesis (DBT) into breast imaging, there has been a significant advancement in the capabilities of Full-Field Digital Mammography (FFDM) for early breast cancer detection. However, the increased use of DBT raises concerns regarding radiation exposure levels.

Objective: This study seeks to determine diagnostic reference levels (DRLs) at the Sultan Qaboos Comprehensive Cancer Care and Research Centre (SQCCCRC) for both FFDM and DBT across different compressed breast thicknesses (CBT), contributing to enhanced understanding of radiation dosimetry in breast

Methodology: Data including average glandular dose (AGD), kVp, mAs, entrance surface dose (ESD) and CBT were retrospectively collected on FFDM and DBT exams. For seven CBT groups ranges from 20 mm to 89 mm, the mean, median, range and 75th percentile of AGD values were determined for craniccaudal (CC) and mediolateral oblique (MLO) views. The differences in AGD values between FFDM and DBT were analyzed, and correlations among AGD and CBT, kVp, mAs and ESD were investigated.

Conclusion: The study confirms that DBT generally results in higher AGD levels than FFDM across various CBT ranges, aligning with those established internationally. This research highlights the need for balancing radiation exposure with diagnostic accuracy in clinical decision-making, reinforcing DBLs as a benchmark for radiation safety in breast cancer screening practice. screening practices.



References:

- Vañó, E., Miller, D. L., Martin, C. J., Rehani, M. M., Kang, K., Rosenstein, M., Ortiz-Loʻpez, P., Mattssc Padovani, R., & Rogers, A. (2017). ICRP Publication 135: Diagnostic Reference Levels in Medical Imaging. An the ICRP, 46(1), 1-144. https://doi.org/10.1177/0164654371717209
- Liu, Q., Suleiman, M. E., McEntee, M. F., & Soh, B. P. (2022). Diagnostic reference levels in digital mammography: a systematic review. Journal of Radiological Protection, 42(1). https://doi.org/10.1088/1361-6498/ac4214.

SUBMISSION OF MANUSCRIPTS

Manuscripts to be considered for publication should be submitted as a WORD document to:

Francis Hasford, Co-editor: haspee@yahoo.co.uk Sameer Tipnis, Co-editor: tipnis@musc.edu

MANUSCRIPT PROPOSALS

Authors considering the development of a manuscript for a Review Article can first submit a brief proposal to the editors. This should include the title, list of authors, an abstract, and other supporting information that is appropriate. After review of the proposal the editors will consider issuing an invitation for a manuscript. When the manuscript is received it will go through the usual peerreview process.